Geoscience Frontiers 7 (2016) 315–334

HOSTED BY

ELSEVIER

Contents lists available at ScienceDirect

China University of Geosciences (Beijing)

Geoscience Frontiers

journal homepage: www.elsevier.com/locate/gsf

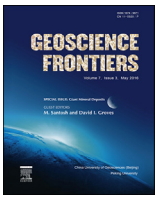

Research paper

From mantle to critical zone: A review of large and giant sized deposits of the rare earth elements

M.P. Smith [a,*], K. Moore [b], D. Kavecsánszki [b], A.A. Finch [c], J. Kynicky [d], F. Wall [b]

[a] School of Environment and Technology, University of Brighton, Lewes Road, Brighton BN2 4GJ, UK
[b] Camborne School of Mines, University of Exeter, UK
[c] Department of Earth and Environmental Sciences, University of St Andrews, UK
[d] Department of Geology and Pedology, Mendel University, Brno, Czech Republic

ARTICLE INFO

Article history:
Received 19 August 2015
Received in revised form
16 December 2015
Accepted 20 December 2015
Available online 12 January 2016

Keywords:
Rare earth elements
Carbonatite
Syenite
Giant deposit
Grade

ABSTRACT

The rare earth elements are unusual when defining giant-sized ore deposits, as resources are often quoted as total rare earth oxide, but the importance of a deposit may be related to the grade for individual, or a limited group of the elements. Taking the total REE resource, only one currently known deposit (Bayan Obo) would class as giant ($>1.7 \times 10^7$ tonnes contained metal), but a range of others classify as large ($>1.7 \times 10^6$ tonnes). With the exception of unclassified resource estimates from the Olympic Dam IOCG deposit, all of these deposits are related to alkaline igneous activity – either carbonatites or agpaitic nepheline syenites. The total resource in these deposits must relate to the scale of the primary igneous source, but the grade is a complex function of igneous source, magmatic crystallisation, hydrothermal modification and supergene enrichment during weathering. Isotopic data suggest that the sources conducive to the formation of large REE deposits are developed in subcontinental lithospheric mantle, enriched in trace elements either by plume activity, or by previous subduction. The reactivation of such enriched mantle domains in relatively restricted geographical areas may have played a role in the formation of some of the largest deposits (e.g. Bayan Obo). Hydrothermal activity involving fluids from magmatic to meteoric sources may result in the redistribution of the REE and increases in grade, depending on primary mineralogy and the availability of ligands. Weathering and supergene enrichment of carbonatite has played a role in the formation of the highest grade deposits at Mount Weld (Australia) and Tomtor (Russia). For the individual REE with the current highest economic value (Nd and the HREE), the boundaries for the large and giant size classes are two orders of magnitude lower, and deposits enriched in these metals (agpaitic systems, ion absorption deposits) may have significant economic impact in the near future.

1. Introduction

The rare earth elements (REE) are currently a focus of global attention because of geopolitical controls on their supply (Hatch, 2012), which have led to them being included in recent and current lists of critical metals (US Department of Energy, 2011; British Geological Survey, 2012; European Commission, 2014). Their importance comes from their use in the production of high strength magnets, fundamental to a range of low carbon energy production approaches, and in a wide range of high technology applications. Reviews are given in Chakhmouradian and Wall (2012), Gunn (2014), and Wall (2014). Production is currently limited to a small number of large deposits (e.g. Bayan Obo, China; Mountain Pass, USA; Mount Weld, Australia; Lovozero, Russia), by-products (e.g. mineral sands, India) or to deposits that have enrichments in specific elements of current high demand, notably dysprosium (Dy), terbium (Tb) and other HREE (e.g. the so called ion absorption deposits in weathered granite of southern China; Kanazawa and Kamitani, 2006). However, a number of deposits are known from relatively recent past production, are currently at the stage of feasibility studies, are at advanced stages of exploration or have been the focus of research. Of these, given the small size of the REE market, most are large enough to have a significant impact on

* Corresponding author.
E-mail address: martin.smith@brighton.ac.uk (M.P. Smith).
Peer-review under responsibility of China University of Geosciences (Beijing).

http://dx.doi.org/10.1016/j.gsf.2015.12.006

global supply, although only Bayan Obo may truly be considered as giant.

The formal definition of a giant ore deposit was proposed by Laznicka (1999) on the basis of the tonnage accumulation index (Laznicka, 1983). This is the amount of metal in a defined ore body divided by its average crustal concentration (or 'Clarke value'). The aim of this was both to show the relative enrichment of different metals in a directly comparative manner, removing the absolute variation of concentration between different metals, and to remove economic bias from discussion of the scale of ore bodies. The latter aim can only ever be partly successful as it is dependent on the cut-off grade used to define an ore body—an inherently economic consideration. However, this approach remains the most clearly defined way to address the problem. Laznicka (1999) defined a giant ore deposits as having a tonnage accumulation index of 1×10^{11}, and a large ore body a tonnage accumulation index of 1×10^{10}. For these values, and using an average REE crustal concentration of 1.5×10^2 ppm (Wedepohl, 1995), a large REE deposit would have 1.7×10^6 tonnes of contained REE_2O_3, and a giant deposit would have 1.7×10^7 tonnes of contained REE_2O_3 (calculated assuming an intermediate atomic mass for REE of 150). The available data for resources in REE deposits from Orris and Grauch (2002) and Long et al. (2010) and other sources are shown in Fig. 1A, and the deposits of large size or greater are shown in Fig. 1B. Because of the current scarcity of data for many of these deposits, resource estimates are commonly not JORC/NI43101 compliant, and for simplicity in this review we have used the figures quoted by those authors. Where compliant data are available they are mentioned below. Of all currently known REE deposits, only Bayan Obo, China, with the ore grade defined at 4.1 wt.% REE_2O_3, counts as

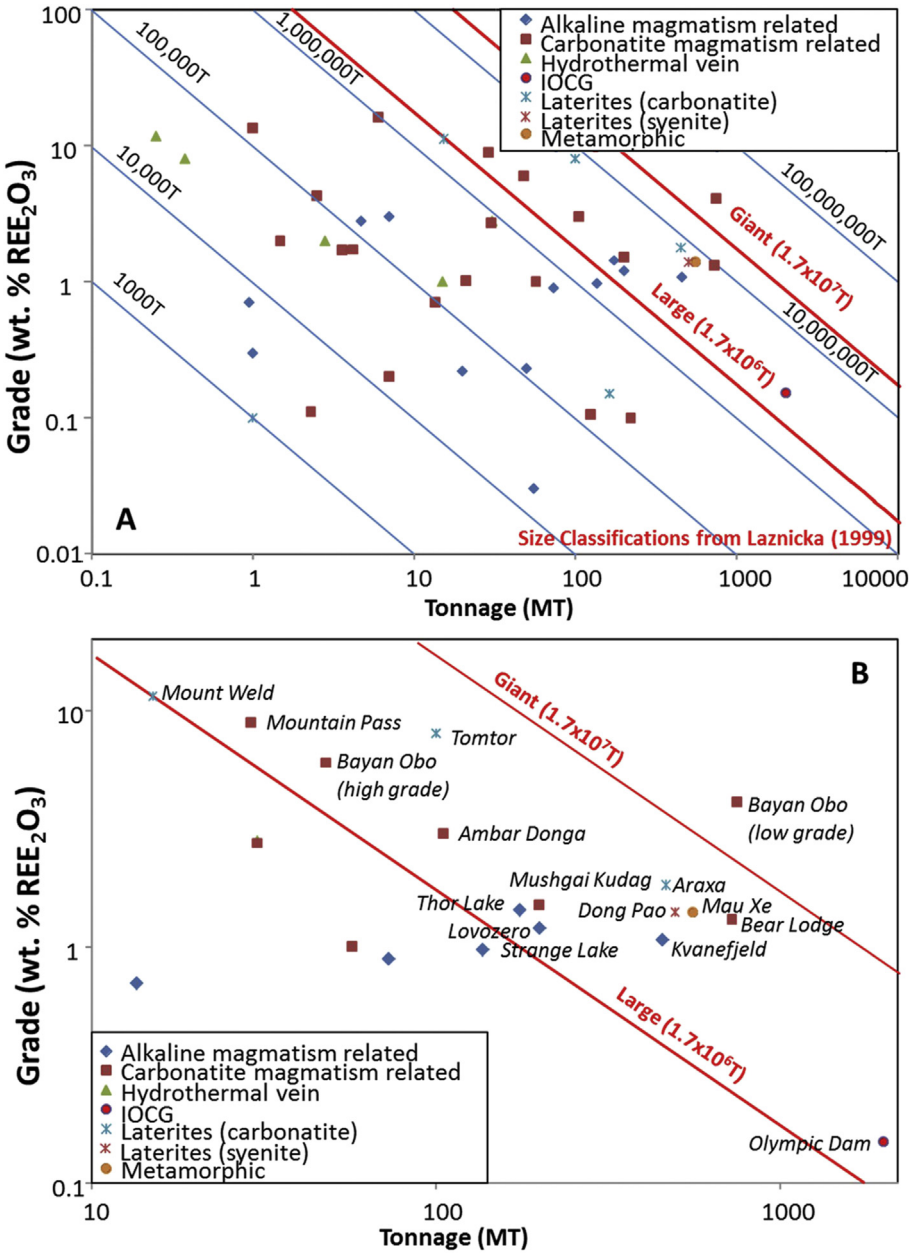

Figure 1. Grade-tonnage plot for resource estimates in REE deposits from Orris and Grauch (2002) and Long et al. (2010). Size classifications after Laznicka (1999) calculated as described in the text.

a truly giant deposit. A number of deposits classify as large, however, and these are likely to have a significant impact on the production of the REE in the near future.

In this paper we review the geological and geochemical characteristics of large and giant REE deposits, and examine the underlying geological controls on the formation of these bodies. It also worth noting, however, that the largest accumulations of the REE are not necessarily those with the greatest potential economic impact. At present, the greatest demand for the REE is for Nd, one of the light REE (LREE) and some of the heavy REE (HREE): Eu, Dy, Tb (HREE defined as REE with atomic mass greater Eu). If the REE are considered as individual elements, rather than as a group, then the corresponding tonnage accumulation indices for the definition of large and giant sized deposits would be reduced by an order of magnitude for the HREE.

2. Deposit types

Rare earth element deposits are developed in virtually all major rock types with examples from igneous, metamorphic and sedimentary (weathering profiles, residual deposits and placers) host rocks (Orris and Grauch, 2002; Long et al., 2010) from settings worldwide (Fig. 2). Large and giant deposits for the whole REE group, however, with the exception of Olympic Dam, are developed in association with alkaline igneous rocks – either carbonatite or syenite. Individual HREE have potentially large deposits *sensu stricto* within the weathered granitoid deposits of SE China (Chi and Tian, 2008).

Carbonatite is an igneous rock with 50 modal% carbonate (*sensu lato*) and containing less than 20 wt.% SiO_2 (Le Maitre et al., 2002), although Mitchell (2005) argued for a broader definition. Mitchell (2005) went on to specify a distinction with genetically related carbothermal residua – that is rocks derived from CO_2-rich hydrothermal fluids. Syenite is an igneous rock with <20 modal% quartz, and alkali feldspar >65% of the total feldspar content (Streckeisen, 1976). Rare earth enrichments are typically associated with quartz-free, feldspathoid syenites. Such rocks are also commonly peralkaline (mole fraction $Na_2O + K_2O > Al_2O_3$) and as such may contain sodic pyroxene (e.g. aegirine) and amphibole (arfvedsonite and riebeckite). Extreme fractional crystallisation of such rocks may lead to molal $(Na_2O + K_2O)/Al_2O_3 > 1.2$, and the formation of complex Zr and Ti minerals such as eudialyte – such rocks are termed agpaitic (Le Maitre, 1989; Sørensen, 1997). Syenites and carbonatites may be related in some composite intrusions, either by extreme differentiation (Wyllie and Tuttle, 1960), or liquid-liquid immiscibility (e.g. Lee and Wyllie, 1998).

Olympic Dam stands alone as the only iron oxide-copper-gold deposit that hosts significant REE mineralisation (Lottermoser, 1995). These REE resources hold currently uneconomic reserve estimates, but may have the potential as by-products in the future. Iron oxide-copper-gold systems are hydrothermal deposits, defined by the dominance of iron oxides rather than sulphide gangues, economic Cu and possibly Au mineralisation, and an association with sodium-rich alteration haloes, and specific trace metal enrichments, including the REE (Hitzman et al., 1992; Williams et al., 2005). The hydrothermal fluids involved are not simply related to coeval magmatic sources, although magmatic-hydrothermal fluids are implicated in the formation of a number of deposits (e.g. Pollard, 2001), and may involve high salinity brines derived from interaction with evaporites, formation waters or highly saline surface waters (Barton and Johnson, 1996, 2000). The characteristics of key large and giant sized deposits are summarised in Table 1.

3. Key large and giant ore deposits

Bayan Obo – The Bayan Obo ore bodies are currently the only known, truly giant sized deposit of the REE. They consist of bastnäsite and monazite developed alongside significant Fe mineralisation in the form of magnetite and hematite (Chao et al., 1997). The ores are hosted within dolomite marble (Le Bas et al., 1997) and may be associated with a local swarm of carbonatite dykes which cut the surrounding Proterozoic metasedimentary sequence and basement Archaean gneiss (Tao et al., 1998; Yang et al., 2011). The mineralisation is associated with alteration of the host dolomite marble to fluorite, apatite, aegirine-augite, riebeckite, arfvedsonite amphibole and barite, with a host of subsidiary REE minerals and related niobium mineralisation. The ores are strongly banded, which Smith et al. (2015) argued was a result of deformation of the ore, possibility intensifying a primary metasomatic banding (Fig. 3A). The banding is cut by veins of aegirine, riebeckite, apatite, calcite and barite associated with further REE mineralisation and the majority of Nb mineralisation. The ores as they now occur are dominantly hydrothermal in origin, but some of the original accumulation may relate to direct magmatic crystallisation from carbonatites intruded into the host marble. The geochronology of the ores is complex, with periods defined from 1230 to 1350 Ma

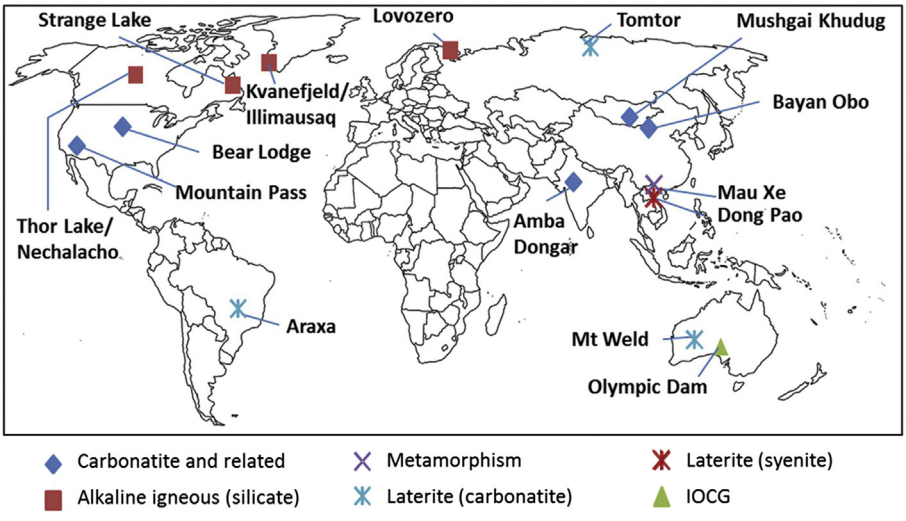

Figure 2. Locations of main large and giant REE deposits mentioned in the text.

Table 1
Approximate resource estimates and description of large and giant REE deposits by the criteria of Laznicka (1999) and as described in the text. Data from Orris and Grauch (2002) and Long et al. (2010), with other references as cited.

Deposit	REE	Grade (wt.%)	Contained REE_2O_3	Location	Description	References
	Tonnage (Mt)		(ppm)			
Carbonatite magmatism related						
Bayan Obo – low grade	750	4.1	30.750	China 41°48′7″N, 109°59′24″E	Metamorphosed, multistage hydrothermal deposit related to several episodes of carbonatite magmatism	Drew et al., 1990; Chao et al., 1997; Wu, 2008; Smith et al., 2015
Bayan Obo – high grade	48	6	2.880			
Bear Lodge Mountains	726	1.306	9.482	USA 44°29′N, 104°27′E	Carbonatites within the Bear Lodge Alkaline complex associated with diatreme breccias	Moore et al., 2015
Amma (Amba) Dongar	105	3	3.150	India 22°N, 72°E	Carbonatite intrusive complex associated with economic hydrothermal fluorite mineralisation, associated with syenites, and intruded in Cretaceous sediments and Deccan Basalt	Viladkar, 1981; Orris and Grauch, 2002; Williams-Jones and Palmer, 2002
Mushgai Khudag	200	1.5	3.000	Mongolia 44°20′N, 104°00′E	Alkaline intrusive complex with alkaline igneous association, carbonatite and nelsonite	Samoylov et al., 1988; Orris and Grauch, 2002
Mountain Pass	29	8.9	2.581	USA 35°29′N, 115°32′E	Carbonatite sill intruded into shonkinite, syenite and granite	Olson et al., 1954; Mariano and Mariano, 2012
Laterite (carbonatite)						
Tomtor	100	8	8.000	Russia 71°00′N, 116°35′E	Deep weathering of multistage alkaline igneous and carbonatite complex (700–410 Ma)	Kravchenko et al., 1996; Orris and Grauch, 2002
Araxa	450	1.8	8.100	Brazil 19°38′N, 46°56′E	Carbonatite intrusive complex associate with alkaline ignenous rocks, intruded into Proterozoic metasediments. Deep weathering with residual enrichment	Traversa et al., 2001; Orris and Grauch, 2002
Mount Weld	15	11.2	1.680	Australia 28°52′S, 122°33′E	Carbonatite intrusive complex intruded into Archaean metavolcano-sedimentary rocks. Deep laterite profile with residual enrichment	Lottermoser, 1990; Orris and Grauch, 2002; Long et al., 2010
Illimausaq (Kvanefjeld; Kringelerne)	457	1.07	4.890	Greenland 60°00′N, 51°12′W	U-REE-Zr deposit in Ilimaussaq alkaline complex	Long et al., 2010; Sørenson et al., 2006
Lovozero	200	1.2	2.400	Russia 67°47′N, 34°45′E	Magmatic and magmatic-hydrothermal mineralisation in nepheline syenite, associated alkaline rocks, alkaline pegmatites and hydrothermal veins	Kogarko et al., 1995; Orris and Grauch, 2002
Strange Lake	137	0.97	1.329	Canada 56°18′N, 64°07′W	Hydrothermally modified pegmatite in Elsonian age peralkaline granite, intruded into Archaean metasedimentary and igneous rocks	Salvi and Williams-Jones, 2006; Long et al., 2010
Thor Lake/Nechalacho	64	1.56	1.000	Canada 62°5′N, 112°37′W	Hydrothermally modified layered syenite intruded into peralkaline intrusive complex	Sheard et al., 2012; Avalon Rare Metals Inc., 2013
Laterites (Syenite)						
Dong Pao	500	1.4	7.000	Vietnam 22°17′N, 103°34′E	Deep weathering of metasomatic mineralisation in Palaeogene syenite and quartz-syenite intruded into Proterozoic metamorphic rocks	Kusnir, 2000; Fujii et al., 2010; Long et al., 2010; USGS, 2015
IOCG						
Olympic Dam	2000	0.15	3.000	Australia 30°27′S, 136°53′E	Proterozoic hydrothermal breccia complex intruded into Proterozoic granitoid. REE mineralisation associated with hematite alteration and Cu mineralisation	Oreskes and Einaudi, 1992; Reynolds, 2000
Metamorphic						
Mau Xe North	557	1.4	7.798	Vietnam 22°29′N, 103°30′E	Metamorphic/metasomatic REE deposit hosted in Carboniferous to Permian marble, limestone, schist. Possible carbonatite affinitiy	Kusnir, 2000; Orris and Grauch, 2002; Long et al., 2010; USGS, 2015

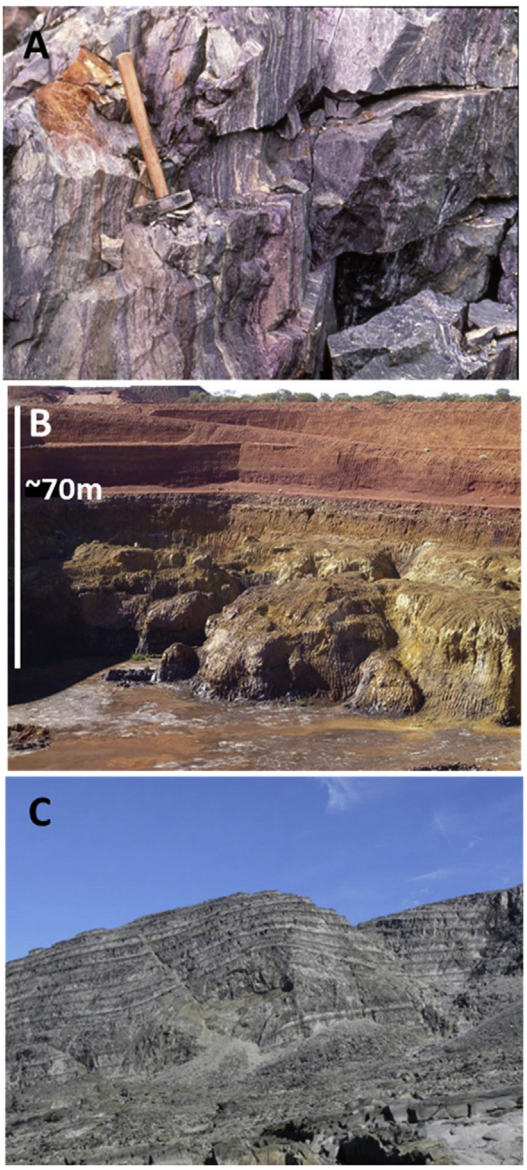

Figure 3. Representative images of REE mineralisation at key deposits. (A) Banded ore from the main pit at Bayan Obo. Bands dominated by fluorite and magnetite are interleaved with those dominated by apatite, monazite and bastnäsite. (B) Laterite developed over carbonatite at Mount Weld, Australia. (C) The Kringlerne layered series in the South of the Ilímaussaq intrusion viewed from the West. The view is approximately 200 m high. Each layer is made of three units rich in: alkali feldspar and nepheline (white, top), eudialyte (red) and alkali amphibole (black, bottom). Each layer is approximately 10 m thick. The layering drapes over a large (~100 m wide) xenolith in the centre of the view.

(largely on Sm-Nd mineral isochrons) and from ~400 to 450 Ma (largely on Th-Pb data for ore minerals; Table 2). Both periods have now been identified from core to rim U-Pb isotope variation in zircon (Campbell et al., 2015), and support interpretations of multistage mineralisation, metamorphism and metasomatic overprint of the ores (Zhang et al., 2003; Smith et al., 2015).

Bear Lodge – The Bear Lodge Carbonatite complex is not currently mined, but hosts potentially economic REE concentrations. The geology of the deposit has recently been reviewed and further studied by Moore et al. (2015). The Bear Lodge Alkaline Complex is part of the Black Hills Intrusive Belt, South Dakota, USA. It consists of a subvolcanic intrusive complex of trachyte, phonolite and latite, with very minor syenite, nepheline syenite and lamprophyre (Staatz, 1983). These are cut by heterolithic, intrusive breccias, which are in turn cut by stockworks of intrusive carbonatite of 52 ± 0.2 Ma age (Anderson et al., 2013), exemplified by the Bull Hill deposit (Moore et al., 2015). The deposit is weathered and oxidised to depths of around 120–180 m. Mineralisation in fresh carbonatite consists of burbankite, early-stage parisite-(Ce) and synchysite-(Ce) with minor bastnäsite-(Ce), which have been affected by multistage hydrothermal alteration to produce secondary fluorcarbonates, ancylite-(Ce) and monazite-(Ce). REE mineralisation in the oxidised zone is dominated by fluorcarbonates, cerianite, and monazite-(Ce) (Moore et al., 2015). The deposit is typically LREE rich, although REE patterns in minerals do vary with paragenesis. Radiogenic isotope systematics of the carbonatite indicate that the source of the magma was in the subcontinental lithospheric mantle, and modified by subduction-related metasomatism, whereas oxygen and carbon stable isotope ratios are consistent with a primary, mantle derived carbonatite, modified by hydrothermal circulation of ultimately meteoric derived waters (Moore et al., 2015).

Araxá – Araxá is a carbonatite intrusion-hosted deposit, which forms part of the Alto Paranaiba Province, southern Brazil (Traversa et al., 2001). It consists of a 4.5 km diameter, circular intrusion, with radial and concentric carbonatite dykes, with mica-rich rocks, phoscorites and lamprophyres, intruding Proterozoic schists and quartzites of the Araxá Group. It has 2.5 km wide, fenite aureole (Traversa et al., 2000; Nasraoui and Waerenborgh, 2001). The complex is inferred to be between 80 and 90 Ma in age (Gibson et al., 1995; references in Traversa et al., 2000). Pyrochlore from Araxá supplies the bulk of the World's niobium. There is also REE mineralisation, dominantly LREE-rich, hosted in monazite, with lesser amounts of burbankite, carbocernaite, ancylite and huanghoite. Monazite and burbankite are apparently magmatic phases, with the hydrothermal formation of carbocernaite and huanghoite, the latter associated with the formation of barite-chalcedony-quartz rock (Traversa et al., 2000).

Amma (Amba) Dongar – The Amba Dongar complex is a carbonatite intrusion associated with the Deccan Volcanic Province, India, and is spatially associated with the extrusion of flood basalts (Williams-Jones and Palmer, 2001). Syenite intrusions occur in the surrounding country rocks (including late Cretaceous sandstone and limestone as well as basalt), whilst the carbonatite consists of concentric rings of carbonatite breccias, calcio-carbonatite and ankeritic carbonatite. The complex hosts large, currently exploited, fluorite deposits (11.6 Mt of 30% CaF_2 – Williams-Jones and Palmer, 2001), but also REE ores of around 105 Mt at 3 wt.% REE_2O_3 (Orris and Grauch, 2002), dominantly in bastnäsite-(Ce) and monazite-(Ce). The surrounding sandstones have undergone extensive potassic fenitisation (Williams-Jones and Palmer, 2001). The carbonatite exsolved a range of aqueous-carbonic solutions, which fenitised the aureole, and later underwent hydrothermal alteration from lower T (<150 °C) meteoric hydrothermal solutions which formed fluorite (Palmer and Williams-Jones, 1996).

Mushgai Khudag – The Mushgai Khudag REE deposit is located in central South Mongolia. It is located in the central part of the Mushgai Khudag volcano-plutonic complex with a central ring structure of almost 30 km in diameter. It is intruded into middle Paleozoic sedimentary and volcanogenic rocks within the Mandal Gobi hills. The REE mineralisation is hosted by late Jurassic (142 ± 3 Ma) alkaline intrusions including syenites, granosyenites porphyries and shonkinite porphyries, which form stocks and/or dikes (Kynicky, 2006; Baatar et al., 2013). Twenty ore bodies have been recognised along the endo- and exocontact parts of syenite and syenite-porphyry bodies. The ore includes mineralised breccia with carbonate cement, mineralised carbonatite, magnetite-apatite ore and complex phosphate ore. Phosphate dominantly occurs in the

Table 2
Summary of mineralogy and geochronology of large and giant REE deposits.

Deposit	Main host minerals	Processes	Age (Ma)	Notes	References
Carbonatite magmatism related					
Bayan Obo	Mon, Bast	Mag?, Ht	1235–1341	Ore Sm-Nd isochrons	Refs. in Smith et al., 2015
		Mag?, Ht	1314 ± 56.5	Ore Zircon concordia (core)	Campbell et al., 2015
		Mag?, Ht	1223–1354	Carbonatite Sm-Nd isochrons	Refs. in Smith et al., 2015
		Mag?, Ht	402–442	Vein Sm-Nd isochrons	Refs. in Smith et al., 2015
		Meta, Ht	398–553	Ore Th-Pb isochrons	Wang et al., 1994
		Meta, Ht	455 ± 28	Ore Zircon concordia (rim)	Campbell et al., 2014
Bear Lodge Mountains	Burb, Par, Synch	Mag, Ht	52 ± 0.2	Ar-Ar biotite + K-feldspar	Anderson et al., 2013
Amba Dongar	Bast, Mon	Mag, Ht	61–76	K-Ar fenite feldspar	Deans et al., 1972
Mushgai Khudag		Mag	138 ± 3	Rb-Sr isochron	Baatar et al., 2013
Mountain Pass	Bast	Mag	1375 ± 5	Th-Pb carbonatite monazite	DeWitt et al., 1987; Castor, 2008
		Mag	1417 ± 4.6	U-Pb zircon	Premo et al., 2013
Laterite (Carbonatite)					
Mount Weld	Mon, Synch (primary),	Mag, Ht	2025 ± 10	Re-Os isochron	Graham et al., 2004
	Mon, Church,	Weath	2380 ± 170	Bulk rock Sm-Nd	Graham et al., 2004
	Plgm (secondary)		2021 ± 13	Rb-Sr isochron	Collerson, 1982
			late Cretaceous–early Cenozoic	Stratigraphic	Graham et al., 2003, 2004
Araxa – total	Mon	Mag, Ht, Weath	80–90	K/Ar, Ar/Ar, U/Pb	Refs. in Traversa et al., 2000
Tomtor	Flor, Mon, Rhab	Mag, Weath	700	Syenite U-Pb zircon	Vladykin et al., 2014
	Xen, Bast		400	Carbonatite Ar-Ar mica	Vladykin et al., 2014
Alkaline magmatism related					
Illimausaq/Kvanefjeld		Mag	1108 ± 21; 1143 ± 20	Rb-Sr whole rock	Wu et al., 2010
		Mag	1168 ± 21	Rb-Sr whole rock	Blaxland et al., 1978
		Mag	1160 ± 2	Rb-Sr whole rock	Waight et al., 2002
Lovozero	Lop	Mag	373 ± 11	U-Pb loparite	Mitchell et al., 2011
		Mag	370 ± 6.7	Rb-Sr whole rock	Kramm and Kogarko, 1994
Strange Lake	All, Gad, Kain, Fluo,	Mag, Ht	1240 ± 2		Miller et al., 1997
	Bast, Gar, Mon	Mag, Ht	1271 ± 30	K-Ar amphibole	Currie, 1985
Thor Lake	Eud, Zir, Ferg, Bast,	Mag, Ht	2094 ± 10	U-Pb zircon	Bowring et al., 1984
	Par, Synch, All				
IOCG					
Olympic Dam	Bast, Flor, Mon, Xen	Ht (IOCG)	1572 ± 99	Sm-Nd isochron	Johnson and McCulloch, 1995
		Ht (IOCG)	1592 ± 8; 1584 ± 20	U-Pb zircon	Johnson and Cross, 1995
		Ht (IOCG)	1590 ± 8; 1577 ± 5	^{207}Pb–^{206}Pb hematite	Ciobanu et al., 2013
Laterites (syenite)					
Dong Pao	Bast	Mag, Weath	Palaoegene	Stratigraphic	Fujii et al., 2010
Metamorphic					
Mau Xe North	Bast, Par, Pyr	Mag?, Meta	30.2 ± 3.4 to 31.6 ± 3.7		Thuy et al., 2014

Mon – Monazite; Bast – Bastnasite; Burb – Burbankite; Par – Parisite; Synch – synchesite; Church – Churchite; Plgm – Plumbogummite; Lop – Loparite; All – Allanite; Gad – Gadolinite; Kain – Kainite; Fluo – Fluocerite; Gar – Garagrinite; Xen – Xenotime; Pyr – Pyrochlore; Rhab – Rhabdophane; Eud – Eudailyte; Zir – Zircon; Ferg – Fergusonite. Dominant formation processes indicated by Mag – magmatic; Ht – Hydrothermal; Weath – Weathering. IOCG denotes Iron oxide copper-gold type deposit.

form of apatite and the REE are mainly hosted in bastnäsite and Ca-REE fluorcarbonates. The complex mineralogy and paragenetic relations of the ore attest to a primary magmatic accumulation modified by hydrothermal processes. Alteration associated with REE mineralisation includes feldspar, apatite, fluorite, celestine, magnetite and barite (Baatar et al., 2013). The resource at Mushgai Khudag has variably been reported as 200 Mt at 1.5 wt.% REE_2O_3, to more recent estimates of 23 Mt at an average grade of ~1 wt.% REE_2O_3 (restricted to the main ore body).

Mountain Pass – The Mountain Pass deposit, California, USA, was the world's largest source of the LREE from the 1960s to the mid-1990s, before closing in 2002 and reopening in 2013. The rare earth ore body is hosted by the Sulphide Queen Carbonatite (Olson et al., 1954). The carbonatite is unusual that it is associated with ultrapotassic alkaline rocks ranging from shonkinite, through syenite to granite (Castor, 2008). These form a group of roughly tabular to lensoid bodies intruded into rocks of the ultrapotassic volcanic belt over ~10 km (Castor, 2008). The main REE mineral in the ore is bastnäsite-(Ce), with minor parisite-(Ce) and monazite-(Ce). The carbonatite overall is unusual in extreme LREE and Ba enrichment and its depletion in Nb and P. The carbonatites have been dated at 1375 ± 5 Ma, approximately 25 Ma younger than the associated ultrapotassic rocks (DeWitt et al., 1987). Bastnäsite and barite both appear to be magmatic phases (Fig. 4) in sövite and dolomitic sövite carbonatites (Castor, 2008). Castor (2008) concluded that, despite apparent age differences, the carbonatites where probably derived from similar magmas to the ultrapotassic suite, ultimately derived from mantle enriched either by metasomatism, or contamination by subducted crustal rocks. A zone of fenitisation surrounds the carbonatite dykes, and fluorite veins are present.

Mount Weld – The Mount Weld deposit, western Australia, is developed in a 70–130 m thick laterite (Fig. 3B) developed on carbonatite bedrock (Duncan and Willett, 1990; Lottermoser, 1990; Hoatson et al., 2011). As well as REE_2O_3 resources of 15 Mt at 11.2 wt.%, it also hosts significant resources of Nb, Ta, Zr, and phosphate. The carbonatite intrudes an Archaean volcano-sedimentary sequence, within the fault bounded Laverton tectonic zone, and has itself undergone greenschist facies metamorphism. It forms part of a Palaeoproterozoic alkaline magmatic province, including kimberlites and other carbonatites (Duncan and Willett, 1990). The lateritic regolith is the host to the main economic REE resources. Primary carbonatite REE minerals and REE-bearing minerals (apatite, monazite-(Ce), synchysite-(Ce)) were broken down during weathering and redeposited in the laterite profile as neoformed apatite and monazite-(Ce), crandallite, goyazite, gorceixite, and florencite-(Ce), with the HREE being particularly concentrated in xenotime-(Y) and churchite-(Y) (Lottermoser and England, 1988; Lottermoser, 1990). There are also REE concentrations in the lacustrine sediments which overly the laterite profile. Radioisotope data indicate the primary carbonatite

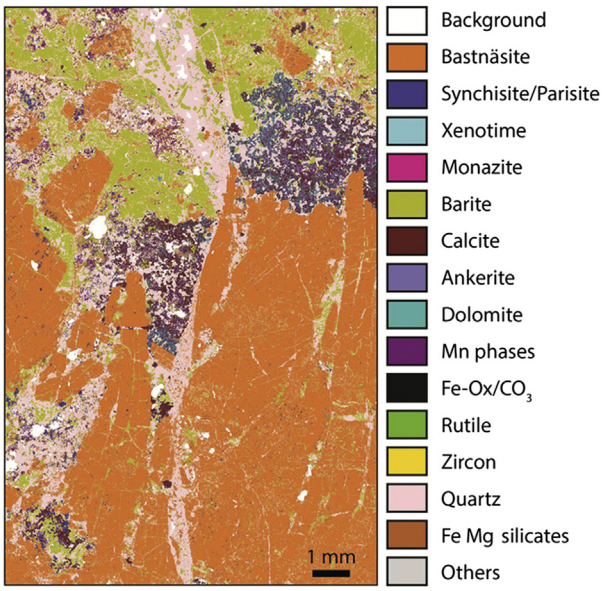

Figure 4. QEMSCAN® false-colour images of REE mineralisation in Mountain Pass carbonatite: primary magmatic bastnäsite is cut by Mn-rich quartz-barite hydrothermal mineralisation with associated synchysite and parisite. QEMSCAN®: quantitative evaluation of minerals using scanning electron microscopy. Details of the analytical technique are reviewed by Haberlah et al. (2011), and Knappett et al. (2011). Image courtesy of G. K. Rollinson, Camborne School of Mines.

was intruded between 2080 and 2100 Ma (Collerson, 1982; Nelson et al., 1988; Graham et al., 2004; Hoatson et al., 2011). The age of lateritic weathering is not known but the overlying lacustrine sediments are inferred to be late Cretaceous to early Cenozoic. Isotopic constraints indicate the primary carbonatite was derived from melting of an enriched mantle source (Graham et al., 2004). The long term leaching and redeposition of the REE by groundwater in the Mesozoic to Cenozoic was critical in REE enrichment to form an economic resource.

Dong Pao – The Dong Pao deposit in North Vietnam is associated with a Palaeogene alkali granite intrusion (Fujii et al., 2010). The age has not yet been accurately determined. The deposit formed in association with carbonatites, but is notably lateritised in the economically extracted parts of the ore (Fujii et al., 2010). Bastnäsite-(Ce) occurs with fluorite and barite in weathered residues and concentrates. The laterite profile is up to 100 m thick, with highest REE grades in a saprolitic zone at ~60 m below surface. Above this is an oxidised laterite zone with pronounced positive and negative Ce anomalies from which the REE have potentially been leached (Fujii et al., 2010). The REE are dominantly hosted in bastnäsite-(Ce).

Ilímaussaq – Ilímaussaq is a subvolcanic igneous complex (Sørenson et al., 2006), part of the Mesoproterozoic Gardar (1300–1150 Ma) Province of South Greenland (see Upton et al., 2003, Upton et al., 2013 for reviews). It represents the products of extended fractionation from an alkali olivine basalt parent in late Gardar times (1160 ± 2 Ma, Waight et al., 2002) and was emplaced as nested peralkaline rocks, cored by an agpaitic magma, which was then cross-cut by late-stage veins and pegmatites. The agpaitic magma had % level Zr and TREE (with significant Nb, Ta), forming feldspathoids, alkali feldspar, alkali pyroxene or amphibole, and the sodium zirconosilicate eudialyte, alongside a plethora of accessories, many of which host REE. The magma had exceptionally low viscosity and, although the exact mechanism remains in debate (cf. Sørenson, 1997; Pfaff et al., 2008; Hunt, 2015), magma chamber processes produced a stratified deposit, rich in sodalite near the roof (North), fine-grained, laminated, rare-element-rich rocks in the centre and spectacular decametre-scale layered rocks (comprising feldspar/nepheline, eudialyte and amphibole rich layers) at the base (South, Fig. 3C). These three sequences are known by the local terms 'naujaite', 'lujavrite' and 'kakortokite' respectively. Although Ilímaussaq contains many REE-enriched minerals, the majority of the rare earth are hosted in rock-forming zirconosilicates, notably eudialyte and steenstrupine. These have complex structures that accommodate different REE in different crystallographic sites, resulting in heavy- or middle-rare earth enriched profiles. The whole complex was subject to post-crystallisation hydrothermal alteration, which modified much of the primary mineralogy and generated families of REE-rich secondary minerals. Ilímaussaq is divided into two licences, covering the north (Kvanefjeld) and south (Kringlerne) of the complex.

Lovozero – The Lovozero nepheline syenite complex on the Kola Peninsula, Russia is the world's largest layered peralkaline syenite intrusion, with an area of 650 km^2 (Kogarko et al., 1995). It has been mined for loparite-(Ce) as a source of Nb and REE since 1951 (Wall, 2014). The only active mine is now an underground operation at Karnarsurt operated by Lovozerskiy Gok. Lovozero is part of the Kola Alkaline Province, which is located in the eastern part of the Baltic Shield and contains many intrusions of alkaline and ultrabasic silicate rocks and carbonatites, including the world's largest nepheline syenite complex at Khibiny (also spelled Khibina). The Kola intrusions range in age from 410 to 362 Ma (Kramm and Sindern, 2004). The Lovozero nepheline syenites are agpaitic, producing, besides nepheline and alkali pyroxenes, a suite of Na and Ti and Zr, silicates, such as eudialyte and lamprophyllite (Chakhmouradian and Zaitsev, 2012), and a huge diversity of minerals in associated highly differentiated pegmatites (Pekov, 2000). The Lovozero complex consists of four stages (Kogarko et al., 1995) including two main intrusions of nepheline syenite. The older, lower and outer nepheline syenite intrusion that accounts for about 80% of the volume of the intrusion is rhythmically layered (Chakhmouradian and Zaitsev, 2012) with repeating layers of foyaite, urtite and lujavrite. The loparite is concentrated through 1600 m of the intrusion in urtite and lujavrite layers. It is a cumulus phase and varies in composition according to the differentiation of the magma (Kogarko et al., 2002). In the final stages of crystallisation the volatile contents became very high and loparite reacted with the residual melt to form an assemblage of barytolamprophyllite, lomonosovite, steenstrupine-(Ce), vuonnemite, nordite-(Ce), nenadkevichite, REE-Sr-rich apatite, vitusite-(Ce), mosandrite, monazite-(Ce), cerite and Ba-Si-rich belovite (Kogarko et al., 2002). The younger, smaller intrusion accounts for about 40% of the surface outcrop and contains eudialyte, with 2–2.5 wt.% REE_2O_3 is also a potential REE ore mineral (Chakhmouradian and Zaitsev, 2012).

Strange Lake – The Strange lake deposit is a Mesoproterozoic, peralkaline granite intrusion, dated at 1240 ± 2 Ma (Miller et al., 1997) and emplaced into paragneiss and quartz monzonitic host rocks, surrounded by fluorite cemented ring breccias (Vasyukova and Williams-Jones, 2014). Potentially economic concentrations of the REE occur within and around pegmatites in the most altered granite, hosted in a wide range of minerals notably including allanite-(Ce), bastnäsite-(Ce), fluocerite-(Ce), gadolinite-(Y), gagarinite-(Y), kainosite-(Y), and monazite-(Ce). Hydrothermal alteration within the pegmatites includes the development of aegirine, and the alteration of zircono- and titano-silicate minerals to gittinsite and titanite alongside hematisation of iron bearing minerals (Salvi and Williams-Jones, 1996, 2006; Gysi and Williams-Jones, 2013; Vasyukova and Williams-Jones, 2014).

Thor Lake/Nechalacho – Thor Lake/Nechalacho is a poly-rare metal (Zr, Nb, REE, Ta, Be, Ga) deposit hosted by nepheline syenite (Sheard et al., 2012). The Nechalacho deposit was formerly

known as the Lake Zone, and occurs as a layered alkaline igneous sequence within the Thor Lake syenite. The syenite forms part of the Blatchford Lake intrusive complex, which was intruded into Archaean mica schists of the Yellowknife Supergroup, between 2185 and 2094 Ma (Sheard et al., 2012). The deposit itself has been dated at 2094 ± 10 Ma (Bowring et al., 1984). The layered complex consists of a sodalite cumulate at its highest level, underlain by pegmatitic syenite with layers of cumulate zircon, and pseudomorphs inferred to be after eudialyte. The LREE are dominantly hosted in monazite-(Ce), allanite-(Ce) and Ca-REE fluorcarbonates. The HREE are hosted in zircon and fergusonite-(Y). At least some of this assemblage was formed by alteration of primary eudialyte, although primary zircon also occurs. There is also evidence for further hydrothermal alteration of zircon by fluoride and carbonate-rich fluids (Sheard et al., 2012; Hoshino et al., 2013). The deposit has significant relative enrichment of the HREE, with up to 27 wt.% HREE oxide relative to total REE oxides. Current measured resources are 10.88 Mt at 1.67% REE_2O_3, with indicated resources of 54.95 Mt at 1.54 wt.% (Avalon Rare Metals Inc., 2013).

Olympic Dam – Olympic Dam is an Iron oxide-copper-gold (IOCG) deposit that forms a world class resource of Cu. In addition, as is typical of this deposit class (Hitzman et al., 1992; Williams et al., 2005), it is anomalously enriched in the REE, in this case enough to constitute a significant, but currently uneconomic, resource, albeit at lower grades than other deposits of comparable levels of contained metal. Early estimates put inferred resources as high as 2000 Mt at 0.15 wt.% REE_2O_3 (Reynolds, 2000), but more recent estimates (marginal and inferred resources) suggest tonnages around 57 Mt, which would place Olympic Dam outside of the large classification of Laznicka (1999). However, the high overall tonnage of the deposit (tonnes at % Cu) and potential for large resources depending on the grade definition mean that Olympic Dam merits mention in this review. The deposit consists of hematite cemented, diatreme, breccias, dominantly of granitic lithologies, but also including clasts of laminated barite, volcanic rocks, other intrusive rocks, vein fragments, and arkosic sediments (Reeve et al., 1990). The REE are primarily present as bastnäsite-(Ce), monazite-(Ce), florencite-(Ce) and xenotime-(Y) (Reynolds, 2000), and increase in concentration with increasing proportions of replacement or matrix hematite in the breccias (Oreskes and Einaudi, 1992). The deposits are inferred to have formed as, potentially magmatic-related, explosion breccias (Oreskes and Einaudi, 1992). U-Pb zircon ages of igneous rocks and mineralisation suggest all activity was broadly coeval, at around 1590 Ma (Hoatson et al., 2011).

Mau Xe North – The Mau Xe North deposit occurs in the Fan Si Pan mountains in the north of Vietnam, approximately 40 km to the north of Dong Pao (Kusnir, 2000). Tabular or lens-form ore bodies are hosted in Permo-Carboniferous limestones of uncertain provenance (potentially carbonatite-related). REE mineralisation is hosted in bastnäsite and parisite, associated with uranopyrochlore, gadolinite, pyrite, apatite and abundant barite and fluorite. The highest grades (4–5 wt.% REE_2O_3) are associated with a weathered zone up to 20 m thick (Kusnir, 2000).

Tomtor – The Tomtor massif is a 300 km^2 ring complex, including nepheline syenite, carbonatite and smaller amounts of alkaline-ultrabasic potassic rocks (dominantly lamproites, but also picritic dykes; Kravchenko, 2003). The intrusion is multistage with alkali syenite and 'barren' carbonatite intruded at about 700 Ma and lamproites and REE, Nb-rich carbonatite at 400 Ma (Vladykin et al., 2014). The Nb-REE deposits are situated within and above a central carbonatite stock (Kravchenko and Pokrovsky, 1995; Kravchenko et al., 1996) and the deposit is divided into two main horizons. The lower ore horizon is up to 300 m thick and contains Nb and P-rich rocks developed from several different original rocks including carbonatites, picrites, various volcanics and the country rocks. The upper horizon is developed in weathered carbonatite and lacustrine sediments, and in part consists of a placer REE deposit, but with evidence for extensive chemical reworking and redeposition of the REE minerals (Kravchenko and Pokrovsky, 1995; Kravchenko et al., 1996; Kravchenko, 2003). The upper horizon is the richest ore zone, and contains REE and Y hosted in florencite/goyazite, monazite-(Ce), rhabdophane, xenotime-(Y), and bastnäsite, with Nb concentrated in pyrochlore, columbite, rutile, and ilmenorutile (Kravchenko and Pokrovsky, 1995) with evidence of biological involvement in the mineral precipitation (Lazareva et al., 2015). The deposit is also noticeable for enrichment in scandium (Sc).

The ion adsorption deposits of South China – The ion adsorption deposits of southern China are not formally large or giant deposits as defined here, as total REE resources. They are however, large deposits for individual HREE, and have global significance in terms of the supply for critical materials as they are currently the principal source for HREE (Chi and Tian, 2008). Resources compliant with international codes are not available for the deposits, but estimates range from ~1 Mt at 0.1 wt.% $TREE_2O_3$ within individual areas to combined resources in excess of 10 Mt, albeit still at low grade (0.05–0.2 wt.% REE_2O_3; Chi and Tian, 2008). At present 90% of the known REE resources are located in Jiangxi, Guangdong and Guangxi provinces where the climate is sub-tropical with annual precipitation of over 1500 mm. The clays formed by lateritic weathering of predominantly felsic granitoid rocks containing accessory REE minerals (Kanazawa and Kamitani, 2006), and occur in weathering profiles up to 30 m thick in geomorphologically defined areas where erosion is minimal (Kynicky et al., 2012). The REE occur dominantly in the clay-rich zones of the laterites, either adsorbed onto the surfaces of kaolinite, halloysite and smectite, or as secondary REE phases.

4. Summary of geochemical characteristics and key processes

4.1. Rare earth element distribution

The REE distribution is represented as summary chondrite normalised (values from Wakita et al., 1971) plots in Fig. 5 for all deposits where data are available. Yttrium is plotted as a pseudo-lanthanide with atomic mass intermediate between Dy and Ho. Carbonatite-related deposits are consistently LREE enriched relative to the HREE, with the most extreme enrichments occurring at Bayan Obo, reflecting peaks in overall grade (Fig. 5A). Variation within the group reflects fractional crystallisation of carbonatite, late stage metasomatic enrichment, or both (e.g. Ambar Donga, Ray et al., 2000). The patterns show little evidence for anomalous behaviour of any REE. In contrast, within the alkali syenites, patterns in the most REE enriched rocks are HREE dominated, although earlier, eudialyte-free rocks (notably at Lovozero; Arzamastsev et al., 2008; Fig. 5B) are relatively LREE enriched, but have lower total REE. The overall trend reflects the extreme fractionation of the agpaitic rocks. This is well illustrated by the analyses of samples from the Strange Lake high grade mineralisation zone (Kerr, 2015) where extreme levels of HREE enrichment are achieved, associated with the development of a marked negative Eu anomaly. It should be noted, however, that these rocks are typically highly heterogeneous and it is difficult to provide full representative bulk rock analyses. Within the Olympic Dam breccia the REE pattern reflects that of the host granitoids, again with the development of Eu anomalies (Oreskes and Einaudi, 1992; Fig. 5C). The large sized lateritised deposits (e.g. Mount Weld Dong Pao) are developed on carbonatite substrates, and thus have very similar REE patterns to the carbonatite group (Fig. 5D). The highest grades reached in laterites, however, are higher than in unweathered carbonatites, reflecting supergene enrichment, and positive and negative Ce

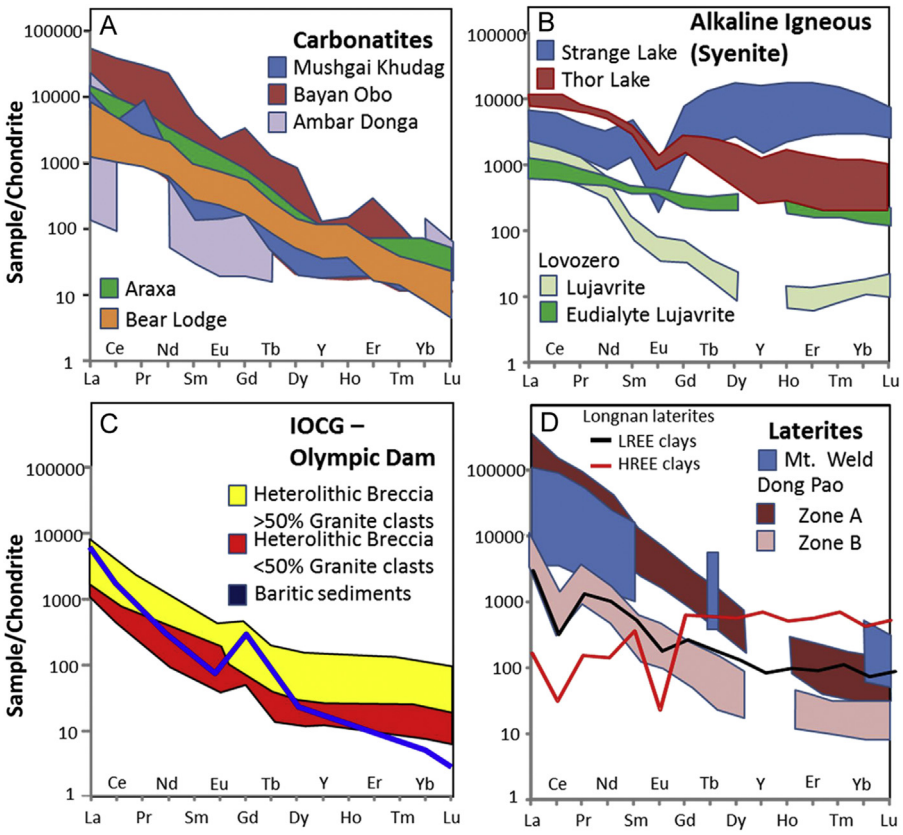

Figure 5. Compilation of representative REE patterns from ores and host rocks classified by deposit type. Data from Oreskes and Einaudi, 1992; Ray et al., 2000; Traversa et al., 2000; Arzamastsev et al., 2008; Fujii et al., 2010; Sheard, 2010; Kynicky et al., 2012; Lai et al., 2012; Baatar et al., 2013; Kerr, 2015; Moore et al., 2015.

anomalies are sporadically developed (notably at Dong Pao; Fujii et al., 2010).

4.2. Temporal distribution

Analysis of the age and rock type data that are available for the large and giant REE deposits (Table 2; Fig. 6A, B) indicates that there are roughly as many deposits hosted in the Phanerozoic as in the Precambrian and that carbonatite-related REE deposits have the highest grade. Despite being small, the sample population appears significant. Approximately two-thirds of carbonatites are Phanerozoic in age (Woolley and Bailey, 2012) but only half of the large and giant carbonatite-related deposits are Phanerozoic and the majority of all dated carbonatites are located in Precambrian cratons (Woolley and Bailey, 2012). The parental magmas for some Paleozoic syenite-hosted REE deposits, e.g. Lovozero, are interpreted as the partial melts of deformed alkaline rocks and carbonatites in a Proterozoic suture zone (Burke and Khan, 2006), and multistage geological histories have been observed in the deposits associated with lithological hosts of greatest antiquity (Smith et al., 2015). The implication is that increasing age and reworking of source mantle may be related to REE concentration (Figs. 6C and 7). The REE deposits associated with felsic silicate rocks, metasomatised and Phanerozoic carbonatites generally have higher tonnage and lower grade than the Precambrian carbonatites. Although the sample size of the population is small, there is a clear trend of increasing REE grades from Phanerozoic back through the Neoproterozoic and Mesoproterozoic to Palaeoproterozoic carbonatites (Fig. 7). Various additional hydrothermal, metamorphic (Bayan Obo) and weathering (Mount Weld and Tomtor) processes have increased the grade of the carbonatite-hosted REE deposits, but do not appear to control the temporal enrichment pattern. This suggests that the parental material of carbonatite-hosted REE deposits must be particularly enriched as an underlying control, or that silicate-hosted REE deposits are the products of extreme differentiation from very large volumes of less enriched alkaline igneous rocks (nepheline syenites).

The Mesoproterozoic represents a peak in formation of the highest grade REE deposits globally (Figs. 6 and 7), distinct from the Phanerozoic peak in carbonatite occurrence that presumably reflects both global evolution of the mantle carbon cycle (Woolley and Bailey, 2012) and the effects of geological preservation (Hawkesworth et al., 2009). The underlying global-scale reasons for REE enrichment must therefore lie within the prevalent mantle-crust and tectonic settings. Studies of strontium, neodymium and lead isotopes (Bell and Blenkinsop, 1987a; Kwon et al., 1989) are in agreement that isotopic ratios for the crust and mantle began to diverge at approximately 3000 to 2900 Ma and correspond to a mean age of melt reservoir formation. The composition of the subcontinental lithospheric mantle changed significantly from the time of the first Archean melt reservoir to the Proterozoic due to extended intervals of metasomatism (Griffin et al., 2003), with enrichment of LREE either slightly before or at the same time as carbonatite magma generation (Bell and Blenkinsop, 1987a). The metasomatism is likely to have been driven by cycles of protracted continental amalgamation, supercontinent break-up and continental reassembly (Casquet et al., 2012), which is temporally associated with the Mesoproterozoic peak in large and giant ore deposits (Fig. 6). Reworking and remelting of deformed alkaline rocks and carbonatites associated with suture zones (Burke and Khan, 2006) can partly explain periodic alkaline magmatism through the geological column at particular localities (Bailey, 1993).

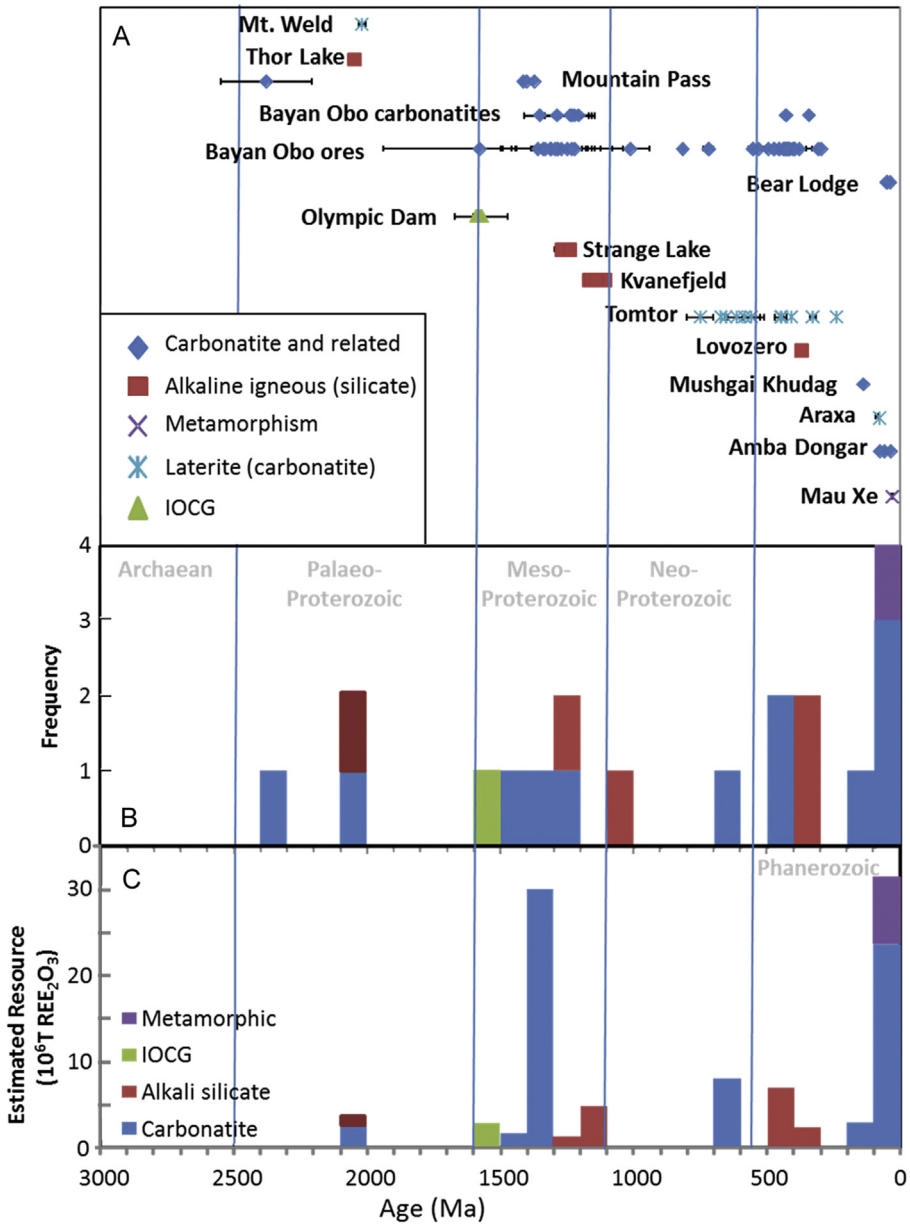

Figure 6. Summary of geochronology of large and giant REE deposits. (A) Summary of individual age determinations (see Table 2 for references). (B) Frequency of occurrence of large and giant deposits by age and deposit type. (C) Distribution of total REE resource with geological time.

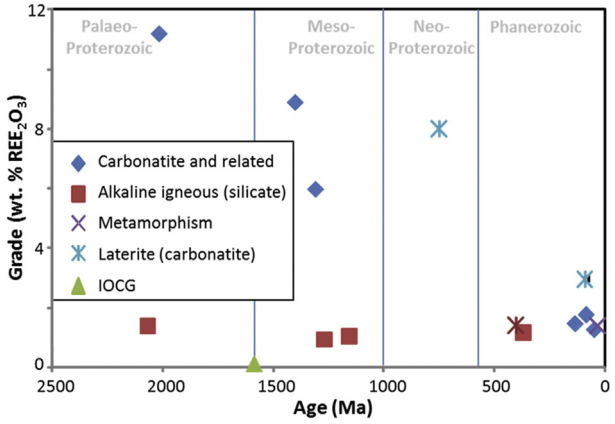

Figure 7. Comparison of deposit age with grade.

It has also been suggested that transfer of stress across plates caused by changes in the configuration of tectonic plates globally, leads to reactivation of tectonic lineaments leading to decompression melting and emplacement of small fraction magmas (Bailey, 1993).

The temporal distribution of mineralisation within individual deposits may also have a role to play in the formation of some of the largest metal accumulations. Bayan Obo is perhaps the clearest example of this, with a multistage geological history defined by a very large number of geochronological studies summarised by Smith et al. (2015). Clear peaks in the distribution of radiometric ages occur at ~1.2–1.3 Ga (Sm-Nd rock and mineral isochrons; e.g. Zhang et al., 2003) and 400–450 Ma (Th-Pb isochrons, Wang et al., 1994; Sm-Nd isochrons from vein minerals, e.g. Hu et al., 2009). Argon isotope geochronology attests to repeated periods of metamorphism in the intervening period (e.g. Ren et al., 1994). Thorium-

Pb Concordia ages from zircon (Campbell et al., 2015) have now indicated cores with ages of 1314 ± 56.5 Ma and rims with ages of 455 ± 28 Ma confirming 2 main periods contributing to metallogeny at the site. Smith et al. (2015) suggested an initial period of alkaline magmatism and carbonatite related mineralisation that was subsequently remobilised during Caledonian metamorphism, possibly with another period of alkaline igneous related fluid flow at this point, indicating reactivation of an enriched mantle source within the new tectonic regime. In a similar way, radiometric age determinations from the Tomtor deposit, for which two stage formation has been proposed on the basis of field relations (pyroxenites, melilites and ijolites, syenites and carbonatites in stage 1; picritic to lamproitic sills and dykes, potassic ultramafic rocks, mineralised carbonate-phosphate tuffs in stage 2), indicate a formation period from 800 to 250 Ma, with possible main stages at 700 and 400 Ma (Vladykin et al., 2014).

4.3. Control from source

A large and diverse body of research has established the ultimate mantle source of carbonatite including those (Simonetti et al., 1995; Xu et al., 2003; Yang et al., 2011; Baatar et al., 2013; Moore et al., 2015) hosting the large and giant REE ore bodies (Fig. 8), and also a mantle contribution to the REE metal flux in the largest hydrothermal deposit types (e.g. Olympic Dam; Johnson and McCulloch, 1995). Alkali syenite-hosted REE deposits such as Lovozero and Ilímaussaq derive from larger fraction magmas that also have a mantle source (Kramm and Kogarko, 1994; Stevenson et al., 1997). The settings and source of some of the carbonatites hosting large and giant REE deposits have been inferred to include:

- Any of rifted, anorogenic, subduction-related, or post-orogenic tectonic settings (Simonetti et al., 1998; Kogarko et al., 2010; Upton et al., 2013; Moore et al., 2015);
- The frequent involvement of plumes, upwelling mantle or plume-modification of lithosphere (Simonetti et al., 1998; Graham et al., 2004; Castor, 2008);
- A ubiquitous need for metasomatism in a non-convective subcontinental lithospheric mantle to provide the initial trace element enrichment.

The available Sr and Nd isotope data for large and giant sized REE deposits are summarised in Table 3. The similarity of Sr-isotopic ratios for carbonatite and alkali-rich silica-undersaturated rocks and basalts (Powell et al., 1966; Bell and Blenkinsop, 1987a, b) suggested an asthenospheric mantle plume source for carbonatites (Menzies, 1987; Kwon et al., 1989; Schleicher et al., 1990). However, coupling of the crust and mantle through time suggested a lithospheric source depleted by crustal extraction (Bell and Blenkinsop, 1987a), and a depleted lithosphere modified by metasomatism was favoured by Meen et al. (1989). Subsequently, mixing lines between HIMU and EMI in African and European carbonatites (Bell and Tilton, 2001; Bell et al., 2004) were attributed to a plume ascending from the deep mantle and the role of continental lithosphere was modified to volatile concentration in the upper levels of the ascending plume. However, the plume model fails to account for rejuvenation of carbonatite magmatism in specific sites at times coincidental with major plate movements (see above), is not always required, and does not always adequately complement the range of igneous products, incompatible element abundances and geophysical characterisation of the mantle-crust system (Peccerillo and Lustrino, 2005). The first point indicates that a decompressional stress model may be required to explain melting in some places of continued carbonatite activity (Bailey, 1993). The source of syenite hosting REE deposits such as at Khibiny and Lovozero has a depleted isotopic mantle signature relative to the carbonatites hosting large and giant REE deposits (Fig. 8) that, coupled to a high rare metal enrichment favours mantle

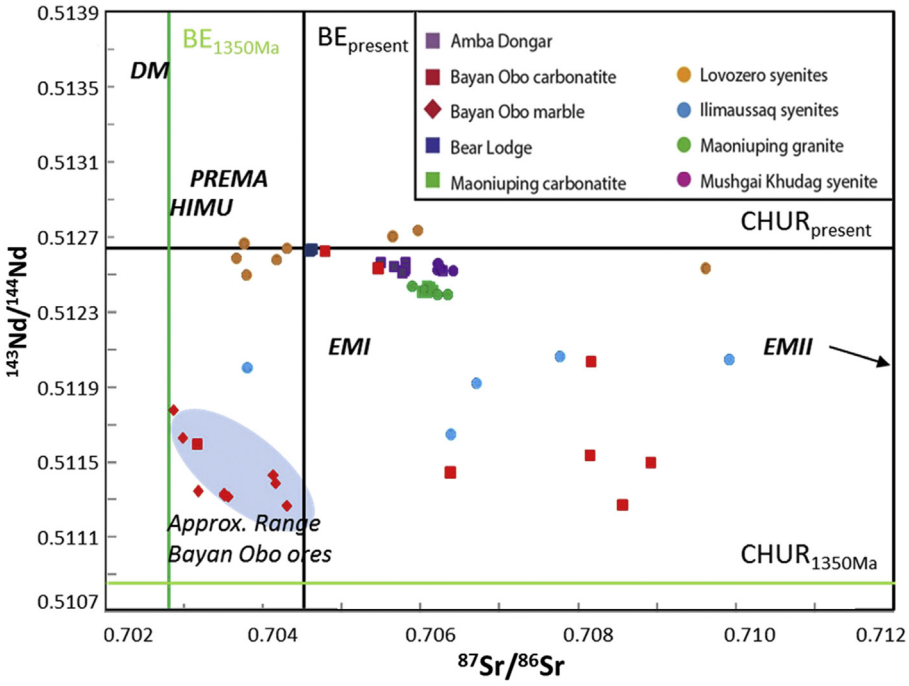

Figure 8. $^{143}Nd/^{144}Nd$ vs. $^{87}Sr/^{86}Sr$ isotope correlation diagram showing mixing between mantle end members in the source region for host rocks to, and minerals within, selected large and giant REE ore deposits. Data for the large and giant ore deposits are from Kramm and Kogarko (1994), Simonetti et al. (1995), Stevenson et al. (1997), Xu et al. (2003), Yang et al. (2011), Baatar et al. (2013), Moore et al. (2015). The mantle reservoirs DM, EMI, EMII, HIMU and PREMA are those of Zindler and Hart (1986). Reference lines are for the Chondrite Normalise Uniform Reservoir (CHUR) and the Bulk silicate Earth (BE), using present day $^{87}Sr/^{86}Sr = 0.7045$ and extrapolated to 1354 Ma (Yang et al., 2011) since the case studies span both the Proterozoic and Phanerozoic, as shown in Table 2.

Table 3
Summary of available strontium and neodymium isotope data from large and giant REE deposits and associated igneous rocks. In this instance lateritised deposits are considered by the original deposit type prior to weathering.

Deposit	$T_{initial}$ (Ma)	ε_{Nd}	ε_{Sr}	References
Carbonatite magmatism related				
Bayan Obo	1235–1341	−8 to +1	−0.41 to 38.84	Refs. in Smith et al., 2014
	1223–1354	−1.7 to −0.5	2.66 to 83.805	Refs. in Smith et al., 2014
	398–553	−18.7 to −10.8		Refs. in Smith et al., 2014
Bear Lodge Mountains	52 ± 0.2	0.2 to 0.6	−1.5 to 2.7	Moore et al., 2014
Amma (Amba) Dongar	61–76	−1.6 to −0.8	15.1 to 19.2	Simonetti et al., 1995
Mushgai Khudag	138 ± 3	−0.34 to −0.35	24.28 to 24.42	Baatar et al., 2013
Mountain Pass	1375 ± 5		22	Premo et al., 2012
	1417 ± 4.6	−1.5 to −6	23.60 to 56.32	Premo et al., 2013
Mount Weld	2025 ± 10	0.61 to 0.49	−2.55 to −0.85	Collerson, 1982; Graham et al., 2003, 2004
Tomtor	700		−3.19 to 0.78	Kravchenko and Pokrovsky, 1995
Alkaline magmatism related				
Illimausaq/Kvanefjeld	1108 ± 21	−1.5 to −2.6	71.02	Wu et al., 2010
	1168 ± 21	−5.9 to 0	−2.34 to 91.52	Blaxland et al., 1978; Stevenson et al., 1997
Lovozero	373 ± 11	+3.8 to + 4.4	−7.29 to −5.45	Mitchell et al., 2011
Strange Lake	1240	−1 to −3		Kerr, 2015
IOCG				
Olympic Dam	1572 ± 99	−4.9 to −0.3	294.1 to 295.2	Johnson and McCulloch, 1995; Varga et al., 2009

metasomatism (Kogarko et al., 2010) as the mechanism for source enrichment for large REE deposits. The radiogenic isotopic evidence for the large and giant REE ore deposits suggests mixing between a mantle source close to HIMU and an EMII (±EMI) component (Fig. 8). The EMII mantle end-member is most likely to represent a subcontinental lithosphere component since the presence of metasomatism in a non-convecting lithospheric mantle is a necessary pre-requisite in all the carbonatite-hosted case studies.

4.4. Magmatic processes

Carbonatites that originate as primary and parental magmas in the mantle are accepted to be small fraction, near-solidus melts that are dolomitic in composition (Wallace and Green, 1988). Where carbonatites that host large REE deposits are associated with pyroxenites (e.g. Araxá), similar REE profiles indicate a single parent magma existed that has evolved through fractional crystallisation of silicate minerals (Traversa et al., 2001). This suggests that the parental magmas to the carbonatites that host some of the large and giant REE ore deposits may contain an appreciable amount of silica. The association of such carbonatites with lamprophyres and kimberlites (e.g. Mount Weld, Bear Lodge) and the isotopic similarity of the sources for carbonatites and syenitic rocks (Fig. 8) further illustrate that a variety of carbonated silicate parental magma compositions can exist in the ultimate mantle source region for the REE ore deposits. A growing body of high pressure experimental research shows that a continuum of compositions is generated with increasing melt fraction, pressure and temperatures, from carbonatites through silicocarbonatite to silicate magmas in the mantle (Girnis et al., 2005; Gudfinnsson and Presnall, 2005; Moore, 2012). Small-fraction melting of mantle metasomes can readily explain the volatile-rich nature of parental magmas and REE-enrichment relative to most mantle-derived basalts (Chakhmouradian and Zaitsev, 2012).

The large and giant REE ore deposits in intrusions evolved from syenitic residual magmas after large fraction melting of mantle (Boily and Williams-Jones, 1994; Marks et al., 2004) and the extreme concentrations of incompatible elements at the Ilímaussaq complex demand that the processes of fractional melting, fluid transport and fractional crystallisation were capable of scavenging and concentrating trace components of the mantle on a very large scale (Upton et al., 2013). Thus it appears that multiple evolutionary routes exist to develop REE ore deposits after melting of a metasomatised mantle, which we can consider as a continuum between the following possible end member scenarios:

- Small fraction melts of metasomatised mantle concentrate REE in the parental magma, which may be sufficiently volatile-rich to readily exsolve a fluid phase that may cause further concentration of the REE (carbonatite-related deposits).
- Large fraction magmas of enriched mantle generate parental magmas in which the REE signature is more diffuse and that require extreme fractional crystallisation to concentrate the REE (alkali syenite-related deposits).

In carbonatites, REE mineral formation usually takes place at the time of emplacement of the carbonatite, however, REE minerals formed by purely igneous processes are rare. The bastnäsite-bearing carbonatite at Mountain Pass has been proposed as magmatic owing to its igneous textures (Mariano, 1989; Castor, 2008) and to experiments that produced a hydroxyl analogue of bastnäsite from a Mountain Pass-like magma composition (Wyllie et al., 1996). Igneous rock textures and mineral assemblages in unweathered carbonatite from drill core at Mount Weld (Fig. 9) can be grouped into those unaffected by subsequent processes and those that have clearly been affected by hydrothermal fluids. Most other carbonatites have evidence of sub-solidus formation and alteration of REE minerals, although there may have been precursor late-stage magmatic minerals, such as burbankite (Wall and Mariano, 1996; Zaitsev et al., 1998), usually forming in pegmatoid transition environments. Carbonatites that contain evidence of rapid eruption form the mantle, e.g. mantle xenoliths, have low REE contents (Woolley and Church, 2005). Magmatic processes are required in order to build up REE concentrations in the magma to levels where they may precipitate REE minerals or exsolve REE-bearing fluids that can then precipitate REE minerals. The two main candidates for this are fractionation or immiscibility. The build-up of REE in magmas during fractionation depends on which rock forming minerals are produced and their partition coefficients. Calcite, dolomite and apatite are the key minerals plus silicates such as forsterite, diopside, phlogopite, with magnetite and accessory minerals such as pyrochlore and monazite. Apatite in carbonatite is reviewed by Hogarth (1989). Partition coefficients for apatite in carbonatite melts have been determined by Klemme and Dalpe (2003) and Hammouda et al. (2010). Fluorapatite can host significant mass % REE in carbonatite and is probably the most important

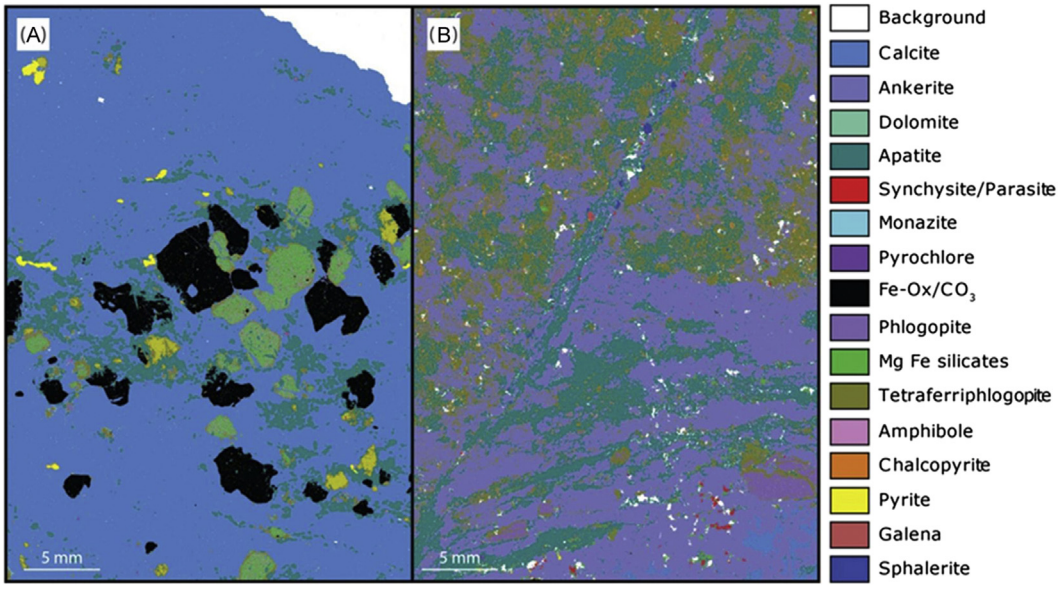

Figure 9. Comparison of magmatic and hydrothermal mineral assemblages and rock textures in QEMSCAN® false-colour images of unweathered carbonatite from drill core beneath the lateritic Mount Weld REE deposits. (A) Magmatic carbonatite with minimal alteration: the mineral assemblage is dominated by calcite, magnetite, olivine and apatite. (B) Hydrothermally altered carbonatite cross-cut by sulphide-bearing vein: apatite is more abundant and iron-rich phlogopite replaces magnetite and olivine in the secondary mineral assemblage, in which REE minerals are dominated by synchysite/parisite. QEMSCAN®: quantitative evaluation of minerals using scanning electron microscopy (Details of the analytical technique are reviewed by Haberlah et al., 2011, and Knappett et al., 2011).

mineral in controlling fractionation of REE. Immiscible separation of carbonate and silicate melts has been discounted as a mechanism to produce REE-rich carbonatite by Veksler et al. (2012), although work by Martin et al. (2013), in highly alkaline hydrous melts shows higher REE concentrations in the carbonate melt.

In general syenite is an evolved alkaline igneous rock, the product of fractionation from an alkaline olivine basalt precursor, ultimately derived from decompression of the underlying mantle (e.g. Upton et al., 2003). Fractionation takes mantle melts, some of which may be relatively enriched in incompatible elements such as REE, and concentrates those elements further in the residual melt. Fractionation of such basalt leads to syenite and nepheline syenite, rocks dominated by alkali feldspar and feldspathoid. Some REE prospects (such as Motzfeldt, South Greenland, McCreath et al., 2013) are hosted by pyrochlore syenite in which LREE substitutes for Ca in the pyrochlore, presumably the result of fractionation of an incompatible element-rich magma. In many large REE deposits hosted by silicate rocks, it is inferred that the impermeable roof zones impeded the loss of volatiles, such that fractionation produced residua which were progressively more volatile rich. Such magmas fractionate beyond syenite to nepheline syenite and, if the conditions allow, further still to peralkaline rocks dominated by alkali mafic minerals (aegirine or arfvedsonite), feldspathoids (usually nepheline and/or sodalite), feldspar (end member Na- and K-feldspar) and a characteristic Ti- or Zr-silicate such as eudialyte. These most evolved rocks have TREE contents in the % levels, with LREE present in apatite-type structures (such as britholite) and HREE in zirconosilicates such as eudialyte. Examples include Ilímaussaq, South Greenland; Nechalacho, Canada; and Lovozero and Khibina in Russia. Agpaitic rocks are also enriched in other rare metals such as Zr, Nb, Ta, Li, making them high-value multi-element deposits.

4.5. Hydrothermal processes

Both carbonatite and evolved nepheline syenite have significant hydrothermal overprints ranging from post-magmatic fluids (e.g. McCreath et al., 2013) to large scale, meteoric convective systems (e.g. Ambar Dongar – Palmer and Williams-Jones, 1996), which enhance or locally remobilise REE. Experimental data on the solubility of REE minerals are relatively limited, but in general REE mineral solubility is enhanced by low pH, high salt concentration (ligand availability) and ligand type (Haas et al., 1996). The effects of temperature (T) may be variable. Monazite has retrograde solubility at low pH (e.g. Wood and Williams-Jones, 1994; Poitrasson et al., 2004; Cetiner et al., 2005), but solubility increases with T at neutral to basic pH (Pourtier et al., 2010). Ligand availability and solute concentration also play a key role, with important REE^{3+} complex ions formed with hydroxide, chloride or fluoride, and possibly sulphate and carbonate, depending on solution composition and pH (Wood, 1990; Haas et al., 1995). High T experimental data are now available for a number of important ligands, including Cl^- and F^- (Gammons et al., 1996; Migdisov et al., 2009), and to some extent SO_4^{2-} (Migdisov and Williams-Jones, 2008). These data have been used to demonstrate that, despite high association constants for REE-F complexes, the combination of strong association of HF at high temperatures, low solubility products for REE-F bearing minerals and the common buffering of F activities to very low levels because of the low solubility of fluorite, the actual role of REE-F complexes in hydrothermal REE transport may be minimal. However, F^- in solution may be significant in causing deposition of REE minerals (Williams-Jones et al., 2012). This means that chloride brines may be the critical agent for hydrothermal REE deposit formation, with a possible role for other ligands (e.g. SO_4^{2-}) in less common or more extreme environments.

Bayan Obo perhaps represents the clearest example of hydrothermal processes in a carbonatite related REE deposit, although details of fluid circulation stages have been obscured by multiple stages of overprinting and metamorphism. The fluids responsible were shown to be variably saline, aqueous-carbonic fluids; Na-rich brines (up to 15 wt.% NaCl eq.); aqueous-carbonic brines which evolved to halite saturated brines and CO_2-rich fluids via immiscibility; and low T (<200 °C), low salinity fluids, possibly of

meteoric derivation that were responsible for the Ba-alteration of the ores (Smith and Henderson, 2000). Primary hydrothermal mineralisation is represented by monazite-(Ce) in dolomite marble (Chao et al., 1997; Smith et al., 1999), which was subsequently altered and overprinted by the development of basnäsite-(Ce). A subsequent, temporally distinct, stage of hydrothermal alteration and mineralisation is indicated by aegirine-reibeckite-fluorite-calcite-barite veins. This late hydrothermal flux clearly added to the Nb content of the ore (Smith and Spratt, 2012), may have added (Yang et al., 2011) and definitely remobilised REE (Smith et al., 2000). In other less deformed, carbonatite-related deposits the relationship between post-magmatic hydrothermal alteration and REE mineralisation is clearer. At Bear Lodge primary REE minerals are replaced by secondary REE fluorcarbonates, ancylite and monazite, and variations in La/Nd ratios, the overall chondrite normalised REE profiles and the oxygen and carbon stable isotope systematics all indicate post-magmatic hydrothermal alteration and the remobilisation of REE. The fluids involved range from fluids derived from magmatic degassing, down to meteoric fluid involved in producing a pervasive hydrothermal overprint (Moore et al., 2015). Similar variations, and the extensive fenitised aureole, have been interpreted in the same way at Araxá (Traversa et al., 2001), whilst alteration has been identified as a key process in ore formation at Mount Weld from fenitisation (Hoatson et al., 2011), and at Mountain Pass from ore alteration mineral assemblages (Olson et al., 1954; Castor, 2008). At Ambar Dongar weakly altered carbonatites contain florencite, alongside minor bastnäsite and parisite, whilst more strongly altered carbonatites contain REE fluorcarbonates in association with barite, fluorite and quartz (Doroshkevich et al., 2009). Initial alteration was by a CO_2-CH_4 bearing S- and K-rich aqueous fluid exsolved from calciocarbonatite. Later fluids, exsolved at shallower intrusive levels, had increasing Cl contents, and were responsible for formation of the fenite aureole. This stage was overprinted Na-Cl bearing fluids of meteoric derivation (Viladkar and Schidlowski, 2000; Williams-Jones and Palmer, 2001) which may have mixed with magmatic waters, and been responsible for the extensive fluoritisation of the deposit (Palmer and Williams-Jones, 1996). Hydrothermal alteration of ore is also clear at Mountain Pass, although less thoroughly investigated. Pervasive quartz alteration can be as high as 60% of the ore in places, mainly replacing calcite, but also barite and bastnäsite, and talc alteration of carbonatite is associated with the formation of allanite (Olson et al., 1954; Castor, 2008) and the sulphide assemblage appears to be hydrothermal in origin. Hydrothermal effects may also have had significant effects at deposits such as Mushgai Khudug (Baatar et al., 2013), and Mount Weld (Hoatson et al., 2011).

Within alkali syenite (Sorensen, 1997), magmatic volatiles contribute to the composition of later hydrothermal solutions. This is true at all the major alkaline silicate complexes (e.g. fluoritisation at Dong Pao; Fujii et al., 2010), but possibly the most detailed investigations of related hydrothermal processes are at Strange Lake. Here, high temperature alteration (>350 °C) leading to the alteration of aegirine to arfvedsonite is attributed to orthomagmatic fluids (Salvi and Williams-Jones, 1990). This fluid is inferred to have high salinity, and co-existed with an immiscible carbonic phase which was involved in redox reactions with Fe oxides resulting in the formation of hydrocarbons (Salvi and Williams-Jones, 2006). This high salinity fluid was responsible for transport and enrichment of Zr, Nb, Y and the REE. Further work has now suggested that Zr was mobilised by HF and HCl-HF bearing brines, down to low temperature (>250 °C), but the REE where dominantly mobilised by Cl-dominated fluids at higher T (~400 °C), as chloride complexes (Gysi and Williams-Jones, 2013). At Lovozero fluid inclusions in lujavrite and other rock types are dominantly carbonic (Potter et al., 2004) in contrast to Ilímaussaq where methane dominates (Konnerup-Madsen and Rose-Hansen, 1982). Although hydrothermal overprinting in alkaline intrusions may increase the REE grade, it can in other cases replace primary REE-bearing minerals with intimate nm-scale intergrowths of secondary minerals that pose a challenge for efficient extraction (McCreath et al., 2013).

4.6. Weathering effects

A number of the largest REE deposits show evidence for significant weathering effects, and in Mount Weld, Tomtor and Dong Pao weathering has contributed to the economic viability of the ore by partial degradation of primary minerals and supergene enrichment resulting in the concentration of REE in secondary minerals. In general REE are leached in the oxidised zones of weathering profiles (zones A and B; the iron crust, and the upper mottled clay layer of laterite profiles) and redeposited in the zone of water table fluctuation (zones B and C; lower mottled clay horizon and saprolite of laterite profiles; e.g. Braun et al., 1993). Despite relatively weak complexation of the REE at low T (Cetiner et al., 2005) by ligands such as Cl^-, the retrograde solubility of monazite under acid conditions and possibility for high activities of carbonate and organic ligands (Wood, 1993; Chen et al., 1998) means there is high potential for REE mobility during weathering. Ceitner and Xiong (2008) concluded from a model soil solution that La^{3+} transport would be dominated by oxalate, sulphate and carbonate species alongside the free ion, although low solubilities were predicted on the basis of monazite as the primary phase in the pH range from 5.5 to 8.5. The existence of soluble, primary fluorcarbonates may be a pre-requisite for high remobilisation of the REE during weathering. In contrast, whilst agreeing that oxalate and citrate are likely to have the highest impact on REE mobility, Goyne et al. (2010) concluded significant breakdown of apatite and monazite as REE hosts.

Of the heavily weathered large to giant sized REE deposits, Mount Weld is possibly the best studied (Duncan and Willett, 1990; Lottermoser, 1990; Hoatson et al., 2011). The deposit consists of a mineralogically and chemically zoned laterite profile, with a sharp, karst-like contact with the underlying carbonatite. Above this is a residual zone enriched in relict igneous minerals by the dissolution of carbonates. This is in turn overlain by a supergene enriched zone, characterised by phosphates, alumina phosphates and crandallite-group minerals alongside Fe and Mn oxides. Very high REE concentrations occur in this zone and the REE are hosted in secondary monazite which, at least in part, replaced apatite. The profile was produced by long term leaching and redeposition by groundwater (Lottermoser, 1990; Hoatson et al., 2011). High carbonate concentrations and widely varying pH contributed to the transport and differential redeposition of the REE (Lottermoser, 1990). Similar processes may have operated at the Dong Pao deposit (Fujii et al., 2010), but in this case REE are mainly hosted in bastnäsite-(Ce). Lateritisation was also a critical process in the Tomtor deposit (Kravchenko and Pokrovsky, 1995; Kravchenko et al., 1996). The lower ore horizon is in situ weathered rock (saprolite) with a previous history of hydrothermal alteration, whilst the upper ore horizon is a lacustrine placer deposit consisting of pyrochlore, phosphates and alumina-phosphates of the REE (Kravchenko and Pokrovsky, 1995). For other deposits, weathering processes have less of a core role in producing economic concentrations, but may influence ore character. For example, at Bear Lodge supergene oxidation may have contributed to increased REE grade and modified mineralogy (deposition of ceriantite, fluorcarbonates and secondary monazite) alongside earlier hydrothermal alteration (Moore et al., 2015). Within the strongly weathered deposits, REE patterns do not show major departures from those in host rocks,

although there may be an increase in grade in some zones, and behave anomalously due to oxidation to Ce^{4+} and retention within the oxidised zone of weathering profiles.

5. Discussion

5.1. An assessment of the criteria defining large and giant REE deposits

The initial definition of large and giant ore deposits here was based on total REE content. Although all the REE are currently undergoing some restriction in supply, global demand is focussed on a more restricted range of elements, notably Nd, Eu, Dy, Tb and Y. These metals have lower concentrations in the crust than La and Ce, that dominate many REE minerals (e.g. Ce 64 ppm, Nd 27 ppm, Dy 3.8 ppm, Tb 0.65 ppm; Wedepohl, 1995), providing the large and giant size boundary classifications to 2.7×10^5 and 2.7×10^6 tonnes for Nd, 3.8×10^4 and 3.8×10^5 tonnes for Dy and 6.5×10^3 and 6.5×10^4 tonnes for Tb; a difference of two orders of magnitude for some elements. Considering critical REE in this way enhances the importance of alkali syenite systems and promotes additional deposits into the large and giant classifications. Nepheline syenite deposits were not until recently considered as potential resources for the REE, mainly because the ore in nepheline syenite deposits are minerals such as eudialyte ($Na_{15}Ca_6(Fe^{2+},Mn^{2+})_3Zr_3[Si_{25}O_{73}](O,OH,H_2O)_3(OH,Cl)_2$) and steenstrupine ($Na_{14}Ce_6(Mn^{2+})_2(Fe^{3+})_2Zr(PO_4)_7Si_{12}O_{36}(OH)_2\cdot 3H_2O$; Wall, 2014). Steenstrupine-(Ce) typically has 31% Ce_2O_3, whilst eudialyte does not have essential REE (although it may host up to 10 wt.% REE_2O_3) compared to ~70% in monazite and bastnäsite. The relative enrichment in HREE (Fig. 5B), however, now makes them very attractive targets.

Equally, the ion absorption deposits of the Longnan district, South China, are not large or giant in size on the basis of total REE resource, but have critical importance in terms of current global supply of the HREE (Kynicky et al., 2012). Grades and tonnages of these deposits are poorly defined but as they supply almost all of the current world HREE demand, and total reserves are estimated to be higher than 8 Mt, albeit at very low grades (Chi and Tian, 2008), the scale of their potential economic impact matches the largest magmatic and hydrothermal REE deposits. These are deposits developed in relatively normal alkaline granitoids, albeit typically with a distinctive accessory REE mineral assemblage, where the REE have been concentrated into an easily leachable form by lateritic weathering processes (Bao and Zhao, 2008). The nature of the easily leachable form is currently under investigation, with early studies suggesting REE sorbed onto clay mineral surfaces but more recent data indicating the presence of microcrystalline phases, including carbonate and fluorcarbonate in the weathering profiles (Chi and Tian, 2008). Thus, for individual HREE the 'critical zone' (i.e. the weathering zone at the interface of geosphere, biosphere, hydrosphere and atmosphere) may ultimately prove to be an area of generation of large and giant sized deposits of the critical REE.

5.2. How do large to giant size REE deposits form?

With the exception of Olympic Dam and the ion adsorption deposits all the large or giant sized REE deposits considered here are related to igneous rocks of alkaline composition. As such, although metamorphic and hydrothermal and weathering effects may be critical in raising grades to commercially extractable levels, and for altering primary mineralogy to more easily processable forms, the key controls on the metal content of REE deposits are the enrichment of the igneous source, and the size of the related igneous system. Grade is a function of all the processes that have affected a deposit, and so although grade seems to correlate with age for carbonatite-related deposits (Fig. 7), this may be a function of time available for metal redistribution by metasomatic processes (e.g. Bayan Obo, Smith et al., 2015), and/or multistage reactivation of REE enriched mantle sources (e.g. Bayan Obo, Yang et al., 2011; Smith et al., 2015) and even perhaps weathering (Mount Weld: Lottermoser, 1990; Tomtor: Kravchenko et al., 1996). Such an effect would be much stronger in carbonatites where both REE minerals and host lithologies are reactive compared to the silicate dominated alkali syenite systems. The amount of contained metal for a given cut-off grade, however, must be a function of how much metal was available, which for both carbonatite and alkali syenite deposits must relate to the size of the original intrusion.

Analysis of the reported size of the outcrops of host igneous rocks does not provide a reliable indication of the relative volumes of magma intruded because: (1) The area encompassed by ring complexes emplaced at shallower levels in the crust (e.g. Mushgai Khudag; Baatar et al., 2013) is not comparable to the outcrop area for deeper erosion levels through cumulate complexes (e.g. Araxa; Woolley, 1986); (2) The cumulate complexes highlight that any reconstruction of original magma volume must rely on assumptions regarding primitive magma composition and the relative volume of silicate (and other) crystallisation products observed (Moore, 2012). The absence of any reconstructions of primary magma volumes and evolutionary paths for carbonatites necessitates that modelling currently provides the most reliable means of interpreting the processes operating in the mantle source region for magmas hosting large and giant REE deposits. Modelling of the progressive modification of mantle from the Archaean onwards shows that Phanerozoic mantle source regions are more metasomatised than Proterozoic mantle sources (Griffin et al., 2003). Given preservation bias, Figs. 6 and 7 indicate that it is likely that the less enriched Mesoproterozoic mantle produced a similar number of large REE deposits to Phanerozoic magmatism. This is explained by non-Uniformitarian modelling of the evolution of the earth that interprets Proterozoic mantle 'overturns' as the result of penetration of subducted plates through mantle phase barriers until 0.7 Ga (Davies, 1995). A correlation exists between the resulting plume events with various types of mineral deposit, including IOCG deposits (Groves et al., 2005) and the large REE deposits generally show a similar but very broad correlation with plumes between 1.0 and 1.7 Ga. High-degree melting caused by slab-induced overturns would extract REE from a larger volume of less metasomatised Precambrian mantle, such that subsequent processes operating over extended time intervals could cause extreme REE enrichment.

Significant volumes of alkali syenite, and ultimately agpaitic magma, require large volumes of alkali basalt which evolve to volatile enriched, syenitic compositions via fractional crystallisation. Large volume fractional melts of enriched sources may be generated in relation to plumes (Simonetti et al., 1998; Graham et al., 2004; Castor, 2008) or enhanced melting of enriched mantle sources (Simonetti et al., 1998; Kogarko et al., 2010; Upton et al., 2013; Moore et al., 2015), with deep melting favouring the development of alkaline basalt magmas. Such activity may also give rise to zones of metasomatically enriched upper asthenosphere or lithosphere and/or elevate geotherms such that small-fraction melting occurs, generating carbonatite in association with fractionated silicate magmas such as syenite. Enriched mantle signatures are observed at Khibina and Lovozero, where sources are trace element enriched, but with depleted mantle isotopic signatures, suggesting mantle metasomatism as a key factor in the evolution of the magma source (Kogarko et al., 2010).

Contrasting mechanisms occur in the generation of the largest carbonatite and alkali syenite related REE deposits. Carbonatites may acquire high REE concentrations at source through lower fraction partial melting of mantle (Bailey, 1993), by silicate-carbonate melt partitioning during liquid-liquid immiscibility (Lee and Wyllie, 1998), or by fractional crystallisation (e.g. Xu et al., 2010). For the first of these the highest REE contents in the melt will be achieved by melting of the most enriched mantle. On the basis of isotopic evidence we have argued that the largest deposits have not derive their REE from asthenospheric mantle, and the melting of metasomatised lithospheric mantle may be important in the generation of the most REE enriched carbonatites. Plume activity may still have a role in driving metasomatism by: (1) recycling deeply subducted enriched mantle; (2) generation of carbon-rich melts and fluids during decompression upwelling; and (3) creation of a thermal and stress regime in the upper mantle conducive to flux of carbon-rich metasomatic agents transporting REE and LILE into non-convecting lithosphere. The generation of an early, trace element enriched lithosphere at around 2900 Ma (Bell and Blenkinsop, 1987a) and extended intervals of metasomatism driven by plumes causing continental break up and reassembly (Griffin et al., 2003; Casquet et al., 2012) coupled with higher heat flows may be responsible for the concentration of REE in Proterozoic magmas. Smaller mantle samples caused by reduced upper mantle heat flows could potentially reduce the REE content of carbonatite-related primary magmas with time.

The activation of low fraction partial melting by decompression related to repeated episodes of continental extension (Bailey, 1993), may lead to repeated cycles of melting of metasomatically enriched mantle sources, progressively enriching a single limited area. Such a mechanism could be envisioned at Bayan Obo, where the original tectonic setting of igneous activity and mineralisation has been proposed to be a continental margin related to the break-up of the supercontinent Columbia from 1.3 to 1.2 Ga (Hou et al., 2008), possibly as a result of plume activity, with the reactivation of metasomatically enriched mantle sources during Caledonian subduction (Wang et al., 1994; Yang et al., 2011; Smith et al., 2015). The same may also be true at Tomtor (Vladykin et al., 2014). The extensional settings in which carbonatite magmatism can occur are more extensive than simple continental extensions, and extend to post-orogenic settings (Chakhmouradian et al., 2008).

Whereas the scale of magmatic activity is critical in the production of sources for large and giant REE deposits, subsequent igneous, hydrothermal and weathering processes are important in the attainment of high grades. Alkaline silicate systems are very specifically REE enriched by extreme fractional crystallisation. Models for the generation of agpaitic magmas involve the fractional crystallisation of alkali basalt or nephelinitic magmas under conditions which prevent volatiles escaping. The retention of volatiles allows magmas to evolve to extreme sodium concentrations, and to very high trace metal enrichments (Sørenson, 1997). Hydrothermal activity is implicated in all deposits to some extent. However, the final high grade of a number of deposits is related to hydrothermal activity, as if the final REE mineralogy which effects whether a deposit can be economically mined and processed. Weathering has equally played a critical role in the concentration of the REE into a more restricted volume at Mount Weld, Tomtor and possibly Dong Pao and Mau Xe, consequently raising grades, the scale of the resource must relate to the scale of the original igneous source rock. Only at Olympic dam, where models of large scale hydrothermal circulation leaching metal from a significant crustal volume have been proposed, does the scale of hydrothermal activity appear to be a critical factor in the final deposit formed (Oreskes and Einaudi, 1992). However, even here the involvement of alkaline mafic magmas as a source for the REE and potentially other metals is implied by Nd isotope data (Johnson and McCulloch, 1995), in contrast to smaller scale and less Cu enriched IOCG type deposits in the same district which have Nd isotope systematics suggestive of crustally derived, granitoid metal sources (Skirrow et al., 2007).

6. Conclusions

What precisely counts as a large or giant sized ore body for the REE is dependent on the size definition used. For total REE content, using the size definitions of Laznicka (1999) only one deposit truly classes as giant in size – Bayan Obo in China. However, a number of other deposits can be classified as large in this sense, although for many the definition of resources and reserves is tentative because of limitations in reliable data and resource assessments. Only a few such deposits are currently mined, but those that are not are currently at the stage of exploration or feasibility study, or in some cases mined for other commodities. The commonality in all these deposits (with the possible exception of Olympic Dam) is an association with alkaline igneous rocks – either carbonatites, syenites or both. The total resource of such deposits must be a function of the size of the parent intrusion, and the availability of enriched mantle sources. This typically limits them to areas of long term, metasomatically enriched, lithospheric mantle. Metasomatism of the lithospheric mantle in this context may be linked to either past plume activity, or to mantle enriched by subduction zone processes. The subsequent tectonic settings of melting range from post-orogenic collapse to lithospheric extension. The formation of enriched mantle domains, means that in some cases repeated tectonic activity over long geological time scales may have generated REE-enriched magmas at widely separated times in spatially restricted areas. Bayan Obo may be the key example of this, with multiple stages of activity, alongside metamorphic and metasomatic reworking, being responsible for the unique scale of the REE resource. Rare earth rich systems appear to have occurred throughout geological time. There do, however, appear to be distinctions in the grade and tonnage of deposits that may reflect the generation of enriched mantle domains in the Proterozoic. Increases in grade may also be related to enrichment of ore zones by the potential hydrothermal and weathering processes in specific deposits. A critical factor in what constitutes a large or giant REE deposit is whether the grade for total REE or individual REE is used to define the size of the resource relative to average crustal values. The HREE are up to two orders of magnitude less abundant than Ce, the most abundant REE. Deposits of Nd, Eu, Dy, Tb and Y in agpaitic nepheline syenites and lateritic weathering profiles may class as large for the individual metals, and may have economic impact in coming years.

Acknowledgements

We would like to thank the Guest Editors of this special issue for the invitation to contribute a paper on the origin of giant and large REE deposits. The comments of the editors and an anonymous referee helped improve this manuscript. MS, AF and FW acknowledge the support of the NERC SoS:RARE consortium grant (NE/M011267/1). D. Kavecsanszki acknowledges the support of a post-graduate fellowship from the College of Engineering, Mathematics and Physical Sciences at the University of Exeter.

References

Anderson, A.K., Cosca, M.A., Larson, P.B., 2013. Timing of carbonatite magmatism in the Bear lodge alkaline complex. Geological Society of America Abstracts with Programs 45, 499.

Arzamastsev, A., Yakovenchuk, V., Pakhomovsky, Y., Ivanyuk, G., 2008. The Khibina and Lovozero Alkaline Massifs: Geology and Unique Mineralization. IGC 33, Excursion Guide No 47, IUGS, 58pp.
Avalon Rare Metals Incorporated, 2013. Project fact sheet. Nechalacho, Thor Lake, 2pp.
Baatar, M., Ochir, G., Kynicky, J., Iizumi, S., Comin-Chiaramonti, P., 2013. Some notes on the Lugin Gol, Mushgai Khudag and Bayan Khoshuu alkaline complexes, Southern Mongolia. International Journal of Geosciences 4, 1200–1214.
Bailey, D.K., 1993. Carbonate magmas. Journal of the Geological Society of London 150, 637–651.
Bao, Z., Zhao, Z., 2008. Geochemistry of mineralization with exchangeable REY in the weathering crusts of granitic rocks in South China. Ore Geology Reviews 33, 519–535.
Barton, M.D., Johnson, D.A., 1996. Evaporitic-source model for igneous-related Fe oxide–(REE-Cu-Au-U) mineralization. Geology 24, 259–262.
Barton, M.D., Johnson, D.A., 2000. Alternative brine sources for Fe-oxide(-Cu-Au) systems: implications for hydrothermal alteration and metals. In: Porter, T.M. (Ed.), Hydrothermal Iron Oxide Copper-gold and Related Deposits: a Global Perspective. Australian Mineral Foundation, Adelaide, pp. 43–60.
Bell, K., Blenkinsop, J., 1987a. Nd and Sr isotopic compositions of East African carbonatites: implications for mantle heterogeneity. Geology 15, 99–102.
Bell, K., Blenkinsop, J., 1987b. Archean depleted mantle: evidence from Nd and Sr initial ratios of carbonatites. Geochimica et Cosmochimica Acta 51, 291–298.
Bell, K., Tilton, G.R., 2001. Nd, Pb and Sr isotope compositions of East African carbonatites: evidence for mantle mixing and plume inhomogeneity. Journal of Petrology 42, 1927–1945.
Bell, K., Castorina, F., Lavecchia, G., Rosatelli, G., Stoppa, F., 2004. Is there a mantle plume below Italy? EOS 85, 541–547.
Blaxland, A.B., van Breemen, O., Emeleus, C.H., Anderson, J.G., 1978. Age and origin of the major syenite centers in the Gardar province of South Greenland: Rb-Sr studies. Bulletin of the Geological Society of America 89, 231–244.
Boily, M., Williams-Jones, A.E., 1994. The role of magmatic and hydrothermal processes in the chemical evolution of the Strange Lake plutonic complex, Quebec-Labrador. Contributions to Mineralogy and Petrology 118, 33–47.
Bowring, S.A., Van Schmus, W.R., Hoffman, P.F., 1984. U-Pb zircon ages from Athapuscow aulacogen, East Arm of Great Slave Lake, N.W.T., Canada. Canadian Journal of Earth Science 21, 1315–1324.
Braun, J.-J., Pagel, M., Herbillon, A., Rosin, C., 1993. Mobilization and redistribution of REEs and thorium in a syenitic lateritic profile: a mass balance study. Geochimica et Cosmochimica Aca 51, 4419–4434.
British Geological Survey, 2012. Risk list 2012: an update to the supply risk index for elements or element groups that are of economic value. British Geological Survey NERC 2012, 12.
Burke, K., Khan, S.D., 2006. A geoinformatics system for global nepheline syenite and carbonatite distribution: testing a Wilson cycle model. Geosphere 2, 53–60.
Campbell, L., Compston, W., Sircombe, K.N., Wilkinson, C.C., 2015. Zircon from the East orebody of the Bayan Obo Fe-Nb-REE deposit, China, and SHRIMP ages for carbonatite-related magmatism and REE mineralization events. Contributions to Mineralogy and Petrology 168, 1041.
Casquet, C., Rapela, C.W., Pankhurst, R.J., Baldo, E., Galindo, C., Fanning, C.M., Dahlquist, J., 2012. Fast sediment underplating and essentially coeval juvenile magmatism in the Ordovician margin of Gondwana, Western Sierras Pampeanas, Argentina. Gondwana Research 22, 664–673.
Castor, S.B., 2008. The mountain pass rare-earth carbonatite and associated ultrapotassic rocks, California. Canadian Mineralogist 46, 779–806.
Ceitner, Z.S., Xiong, Y., 2008. Chemical controls on the solubility, speciation and mobility of lanthanum at near surface conditions: a geochemical modeling study. Applied Geochemistry 23, 2301–2315.
Cetiner, Z.S., Wood, S.A., Gammons, C.H., 2005. The aqueous geochemistry of the rare earth elements and yttrium. Part XV. The solubility of rare earth element phosphates from 23 to 150 °C. Chemical Geology 21, 147–169.
Chakhmouradian, A., Wall, F., 2012. Rare earth elements: minerals, mines, magnets (and more). Elements 8, 333–340.
Chakhmouradian, A.R., Zaitsev, A.N., 2012. Rare earth mineralization in igneous rocks: sources and processes. Elements 8, 347–353.
Chakhmouradian, A.R., Mumin, A.H., Demény, A., Elliott, B., 2008. Postorogenic carbonatites at Eden Lake, Trans-Hudson Orogen (northern Manitoba, Canada): geological setting, mineralogy and geochemistry. Lithos 103, 503–526.
Chao, E.C.T., Back, J.M., Minkin, J.A., Tatsumoto, M., Wang, J., Conrad, J.E., McKee, E.H., Hou, Z.L., Meng, Q.R., Huang, S.G., 1997. The sedimentary carbonate-hosted giant Bayan Obo REE–Fe–Nb ore deposit of Inner Mongolia, China: a corner stone example for giant polymetallic ore deposits of hydrothermal origin. USGS Bulletin 2143, 65.
Chen, Z.C., Yu, S.J., Fu, Q.C., Chenm, B.H., Zhang, L.J., 1998. Organic metallogeny of weathering crust RE deposit. Journal of Rare Earths 16, 59–67.
Chi, R., Tian, J., 2008. Weathered Crust Elution-deposited Rare Earth Ores. Nova Science Publishers, New York, p. 308.
Ciobanu, C.L., Wade, B.P., Cook, N.J., Mumm, A.S., Giles, D., 2013. Uranium-bearing hematite from the Olympic Dam Cu-U-Au deposit, South Australia: A geochemical tracer and reconnaissance Pb-Pb geochronometer. Precambrian Research 238, 129–147.
Collerson, K.D., 1982. Age and strontium isotope systematics of the Mt. Weld carbonatite, Western Australia. Report to Union Oil Development Corporation.
Currie, K.L., 1985. An unusual peralkaline granite near Lac Brisson, Quebec–Labrador. Geological Survey of Canada Report 85-1A, 73–90.
Davies, G.F., 1995. Punctuated tectonic evolution of the earth. Earth and Planetary Science Letters 136, 363–379.
Deans, T., Sukheswala, R.N., Sethna, S.F., Viladkar, S.G., 1972. Metasomatic feldspar rocks potash fenites associated with the fluorite deposits and carbonatites of Amba Dongar, Gujarat, India. Transactions of the Institute of Mining and Metallurgy, Section B 81, B1–B9.
DeWitt, E., Kwak, L.M., Zartman, R.E., 1987. U–Th–Pb and $^{40}Ar/^{39}Ar$ dating of the mountain pass carbonatite and alkalic igneous rocks, southeastern California. Geological Society of America Abstracts with Programs 19 (1), 642.
Doroshkevich, A.G., Viladkar, S.G., Ripp, G.S., Burtseva, M.V., 2009. Hydrothermal REE mineralization in the Amba Donga carbonatite complex, Gujarat, India. Canadian Mineralogist 47, 1105–1116.
Drew, L.J., Meng, Q., Sun, W., 1990. The Bayan Obo iron-rare earth–niobium deposits, Inner Mongolia, China. Lithos 26, 46–65.
Duncan, R.K., Willett, G.C., 1990. Mount Weld carbonatite. In: Hughes, F.E. (Ed.), Geology of Mineral Deposits of Australia and Papua New Guinea, Australasian Institute of Mining & Metallurgy, 14. Monograph, Melbourne, pp. 591–597.
European Commission, 2014. Report on Critical Raw Materials for the EU. Report of the Ad Hoc Working Group on Defining Critical Raw Materials. European Commission, 41pp.
Fujii, N., Miyauchi, K., Shukuwa, R., Kusano, T., Miyagawa, H., Ujihara, M., Tanaka, M., 2010. Investigation of geological characteristic and development of processing tests and mining plans for the Dong Pao rare earth deposit in Vietnam. Shigen-Chishitsu 60 (2), 59–70 (in Japanese with English abstract).
Gammons, C.H., Wood, S.A., WilliamsJones, A.E., 1996. The aqueous geochemistry of the rare earth elements and yttrium .6. Stability of neodymium chloride complexes from 25 to 300 degrees C. Geochimica et Cosmochimica Acta 60, 4615–4630.
Gibson, A.S., Thompson, R.N., Leonardos, O.H., Dickin, A.P., Mitchell, J.B., 1995. The Late Cretaceous impact of the Trindade mantle plume; evidence from large-volume mafic, potassic magmatism in SE Brazil. Journal of Petrology 36, 189–229.
Girnis, A.V., Bulatov, V.K., Brey, G.P., 2005. Transition from kimberlite to carbonatite melt under mantle parameters: an experimental study. Petrology 13, 1–15.
Goyne, K.W., Brantley, S.L., Chorover, J., 2010. Rare earth element release from phosphate minerals in the presence of organic acids. Chemical Geology 278, 1–14.
Graham, S., Lambert, D., Shee, S., 2004. The petrogenesis of carbonatite, melonite and kimberlite from the Eastern Goldfield Province, Yilgarn Craton. Lithos 76, 519–533.
Griffin, W.L., O'Reilly, S.Y., Abe, N., Aulbach, S., Davies, R.M., Pearson, N.J., Doyle, B.J., Kivi, K., 2003. The origin and evolution of archean lithospheric mantle. Precambrian Research 127, 19–41.
Groves, D.I., Vielreicher, R.M., Goldfarb, R.J., Condie, K.C., 2005. Controls on the heterogeneous distribution of mineral deposits through time. In: McDonald, I., Boyce, A.J., Butler, I.B., Herrington, R.J., Polya, D.A. (Eds.), Ore Depoits and Earth Evolution. Geological Society Special Publications 248, pp. 71–101.
Gudfinnsson, G.H., Presnall, D.C., 2005. Continuous gradations among primary carbonatitic, kimberlitic, melilititic, basaltic, picritic, and komatiitic melts in equilibrium with garnet lherzolite at 3-8 GPa. Journal of Petrology 46, 1645–1659.
Gunn, G., 2014. Critical Metals Handbook. Wiley, British Geological Survey. American Geophysical Union, p. 454.
Gysi, A.P., Williams-Jones, A.E., 2013. Hydrothermal mobilization of pegmatite-hosted REE and Zr at Strange Lake, Canada: a reaction path model. Geochimica et Cosmochimica Acta 122, 324–352.
Haas, J.R., Shock, E.L., Sassani, D.C., 1995. Rare earth elements in hydrothermal systems: estimates of standard partial molal thermodynamic properties of aqueous complexes of the REE at high pressures and temperatures. Geochimica et Cosmochimica Acta 59, 4329–4350.
Haberlah, D., Strong, C., Pirrie, D., Rollinson, G.K., Gottlieb, P., Botha, P.W.S.K., Butcher, A.R., 2011. Automated petrography applications in quaternary science. Quaternary Australia 28, 3–12.
Hammouda, T., Chantel, J., Devidal, J.L., 2010. Apatite solubility in carbonatitic liquids and trace element partitioning between apatite and carbonatite at high pressure. Geochimica et Cosmochimica Acta 74, 7220–7235.
Hatch, G.P., 2012. Dynamics in the global market for rare earths. Elements 8, 341–346.
Hawkesworth, C.J., Cawood, P.A., Kemp, A.I.S., Storey, C., Dhuime, B., 2009. A matter of preservation. Science 323, 49.
Hitzman, M.W., Oreskes, N., EInaudi, M., 1992. Geological characteristics and tectonic setting of proterozoic iron oxide (Cu-U-Au-REE) deposits. Precambrian Research 58, 241–287.
Hoatson, D., Jaireth, S., Miezitis, Y., 2011. The major rare-earth-element deposits of Australia: geological setting, exploration, and resources. Geoscience Australia 204.
Hogarth, D.D., 1989. Pyrochlore, apatite and amphibole: distinctive minerals in carbonatite. In: Bell, K. (Ed.), Carbonatites: Genesis and Evolution. Unwin Hyman Ltd, London, pp. 105–148.
Hoshino, M., Watanabe, Y., Murakami, H., Kon, Y., Tsunematsu, M., 2013. Formation process of zircon associated with REE-fluorocarbonate and niobium minerals in the Nechalacho REE deposit, Thor Lake, Canada. Resource Geology 63, 1–26.

Hou, G.T., Santosh, M., Qian, X.L., Lister, G.S., Li, J.H., 2008. Tectonic constraints on 1.3–1.2 Ga final breakup of Columbia supercontinent from a giant radiating dyke swarm. Gondwana Research 14, 561–566.
Hu, F.F., Fan, H.R., Liu, S., Yang, K.F., Chen, F., 2009. Samarium-Neodymium and Rubidium-strontium isotopic dating of Veined REE mineralization for the Bayan Obo REE-Nb-Fe deposit, Northern China. Resource Geology 59, 407–414.
Hunt, E.J., 2015. Magma Chamber Dynamics in the Peralkaline Magmas of the Kakortokite Series, South Greenland. Unpublished PhD Thesis. University of St Andrews, UK.
Johnson, J.P., Cross, K.C., 1995. U-Pb geochronological constraints on the genesis of the Olympic Dam Cu-U-Au-Ag deposit, South Australia. Economic Geology 90, 1046–1063.
Johnson, J.P., McCulloch, M.T., 1995. Sources of mineralizing fluids for the Olympic Dam deposit (South Australia): Sm-Nd isotope constraints. Chemical Geology 121, 177–199.
Kanazawa, Y., Kamitani, M., 2006. Rare earth minerals and resources in the world. Journal of Alloys and Compounds 408–412, 1339–1343.
Kerr, A., 2015. Sm–Nd Isotopic Geochemistry of Rare-earth-element (REE) Mineralization and Associated Peralkaline Granites of the Strange Lake Intrusion, Labrador. Current Research (2015) Newfoundland and Labrador Department of Natural Resources, Geological Survey, Report 15-1, pages 63–83.
Klemme, S., Dalpe, C., 2003. Trace-element partitioning between apatite and carbonatite melt. American Mineralogist 88 (4), 639–646.
Knappett, C., Pirrie, D., Power, M.R., Nikolakopoulou, I., Hilditch, J., Rollinson, G.K., 2011. Mineralogical analysis and provenancing of ancient ceramics using automated SEM-EDS analysis (QEMSCAN®): a pilot study on LB I pottery from Akrotiri, Thera. Journal of Archaeological Science 38, 219–232.
Kogarko, L.N., Kononova, V.A., Orlova, M.P., Woolley, A.R., 1995. Alkaline Rocks and Carbonatites of the World, Part Two: Former USSR. Chapman & Hall, London, p. 226.
Kogarko, L.N., Williams, C.T., Woolley, A.R., 2002. Chemical evolution and petrogenetic implications of loparite in the layered, agpaitic Lovozero complex, Kola Peninsula, Russia. Mineralogy and Petrology, 741–724.
Kogarko, L.N., Lahaye, Y., Brey, G.P., 2010. Plume-related mantle source of supergiant rare metal deposits from the Lovozero and Khibina massifs on the Kola Peninsula, Eastern part of Baltic Shield: Sr, Nd and Hf isotope systematics. Mineralogy and Petrology 98, 197–208.
Konnerup-Madsen, J., Rose-Hansen, J., 1982. Volatiles associated with alkaline igneous activity: fluid inclusions in the Ilímaussaq intrusion and the Gardar granitic complexes (south Greenland). Chemical Geology 37, 79–93.
Kramm, U., Kogarko, L.N., 1994. Nd and Sr isotope signatures of the Khibina and Lovozero agpaitic centres, Kola Alkaline Province, Russia. Lithos 32, 225–242.
Kramm, U., Sindern, S., 2004. Timing of Kola ultrabasic, alkaline and phoscorite-carbonatite magmatism. In: Wall, F., Zaitsev, A.N. (Eds.), Phoscorites and Carbonatites from Mantle to Mine: the Key Example of the Kola Alkaline Province, Mineralogical Society Series, 10. Mineralogical Society, London, pp. 75–97.
Kravchenko, S.M., 2003. Porphyric alkaline-ultrabasic potassic rocks of the central Tomtor Massif (Arctic Siberia): carbonatized lamproites. Geologiya i Geofizika 44, 906–918.
Kravchenko, S.M., Pokrovsky, B.G., 1995. The Tomtor alkaline ultrabasic massif and related REE-Nb deposits, northern Siberia. Economic Geology 90, 676–689.
Kravchenko, S.M., Laputina, I.P., Kataeava, Z.T., Krasilnikova, I.G., 1996. Geochemistry and genesis of rich Sc-REE-Y-Nb ores at the Tomtor deposit, northern Siberian platform. Geokhimiya 10, 938–956.
Kusnir, I., 2000. Mineral resources of Vietnam. Acta Montanistica Slovaca 5, 165–172.
Kwon, S.T., Tilton, G.R., Grunenfelder, M.H., 1989. Pb isotope relationships in carbonatites and alkaline complexes: an overview. In: Bell, K. (Ed.), Carbonatite: Genesis and Evolution. Unwin Hyman, London, pp. 360–387.
Kynicky, J., 2006. Carbonatites of South Mongolia. PhD Thesis. Mendel University, Brno, p. 181.
Kynicky, J., Smith, M.P., Xu, C., 2012. Diversity of rare earth deposits: the key example of China. Elements 8, 361–367.
Lai, X.D., Yang, X.Y., Sun, W.D., 2012. Geochemical constraints on genesis of dolomite marble in the Bayan Obo REE-Nb-Fe deposit, Inner Mongolia: implications for REE mineralization. Journal of Asian Earth Sciences 57, 90–102.
Lazareva, E.V., Zhmodik, S.M., Dobretsov, N.L., Tolstov, A.V., Shcherbov, B.L., Karmanov, N.S., Gerasimov, E.Yu, Bryanskaya, A.V., 2015. Main minerals of abnormally high-grade ores of the Tomtor deposit (*Arctic Siberia*). Russian Geology and Geophysics 56, 844–873.
Laznicka, P., 1983. Giant ore deposits: a quantitative approach. Global Tectonics and Metallogeny 2, 41–63.
Laznicka, P., 1999. Quantitative relationships among giant deposits of metals. Economic Geology 94, 455–473.
Le Bas, M.J., Spiro, B., Yang, X., 1997. Oxygen, carbon and strontium isotope study of the carbonatitic dolomite host of the Bayan Obo Fe–Nb–REE deposit, Inner Mongolia, N. China. Mineralogical Magazine 61, 531–541.
Lee, W.J., Wyllie, P.J., 1998. Processes of crustal carbonatite formation by liquid immiscibility and differentiation, elucidated bymodel systems. Journal of Petrology 39, 2005–2013.
Long, K.R., Van Gosen, B.S., Foley, N.K., Cordier, D., 2010. The Principal Rare Earth Elements Deposits of the United States – a Summary of Domestic Deposits and a Global Perspective. US Geological Survey Scientific Investigations Report 2010–5220, p. 96.
Lottermoser, B.G., 1990. Rare-earth element mineralisation within the Mt. Weld carbonatite laterite, Western Australia. Lithos 24, 151–167.
Lottermoser, B.G., 1995. Rare earth element mineralogy of the olympic dam Cu-U-Au-Ag deposit, Roxby Downs, South Australia: implications for ore genesis. Neues Jahrbuch fur Mineralogie Monatshefte 8, 371–384.
Lottermoser, B.G., England, B.M., 1988. Compositional variation in pyrochlores from the Mt Weld carbonatite laterite, Western Australia. Mineralogy and Petrology 38, 37–51.
Le Maitre, R.W., Streckeisen, A., Zanettin, B., Le Bas, M.J., Bonin, B., Bateman, P., Bellieni, G., Dudek, A., Efremova, S., Keller, J., Lamere, J., Sabine, P.A., Schmid, R., Sørenson, H., Woolley, A.R. (Eds.), 2002. Igneous Rocks: a Classification and Glossary of Terms, Recommendations of the International Union of Geological Sciences, Subcommission of the Systematics of Igneous Rocks. Cambridge University Press.
Mariano, A.N., 1989. Nature of economic mineralization in carbonatites and related rocks. In: Bell, K. (Ed.), Carbonatites: Genesis and Evolution. Unwin Hyman Ltd, London, pp. 149–176.
Mariano, A.N., Mariano Jr., A., 2012. Rare earth mining and exploration in North America. Elements 8, 369–376.
Marks, M., Halama, R., Wenzel, T., Markl, G., 2004. Trace element variations in clinopyroxene and amphibole from alkaline to peralkaline syenites and granites: implications for mineral-melt trace-element partitioning. Chemical Geology 211, 185–215.
Martin, L.H.J., Schmidt, M.W., Mattsson, H.B., Guenther, D., 2013. Element partitioning between immiscible carbonatite and silicate melts for dry and H_2O-bearing systems at 1-3 Gpa. Journal of Petrology 54, 2301–2338.
McCreath, J.A., Finch, A.A., Herd, D.A., Armour-Brown, A., 2013. Geochemistry of pyrochlore minerals from the Motzfeldt Center, South Greenland: the mineralogy of a syenite-hosted Ta, Nb deposit. American Mineralogist 98, 426–438.
Meen, J.K., Ayers, J.C., Fregeau, E.J., 1989. A model of mantle metasomatism by carbonated alkaline melts: trace element and isotopic compositions of mantle source regions of carbonatite and other continental igneous rocks. In: Bell, K. (Ed.), Carbonatites – Genesis and Evolution. Unwin Hyman, London, pp. 464–499.
Menzies, M., 1987. Alkaline rocks and their inclusions: a window on the Earth's interior. In: Fitton, J.G., Upton, B.G.J. (Eds.), Alkaline Igneous Rocks. Geological Society Special Publication No. 30, pp. 15–27.
Migdisov, A.A., Williams-Jones, A.E., 2008. A spectrophotometric study of Nd(III), Sm(III) and Er(III) complexation in sulfate-bearing solutions at elevated temperatures. Geochimica et Cosmochimica Acta 72, 5291–5303.
Migdisov, A.A., Williams-Jones, A.E., Wagner, T., 2009. An experimental study of the solubility and speciation of the rare earth elements (III) in fluoride- and chloride-bearing aqueous solutions at temperatures up to 300 °C. Geochimica et Cosmochimica Acta 73, 7087–7109.
Miller, R.R., Heaman, L.M., Birkett, T.C., 1997. U-Pb zircon age of the Strange Lake peralkaline complex: implications for mesoproterozoic peralkaline magmatism in north-central Labrador. Precambrian Research 81, 67–82.
Mitchell, R.H., 2005. Carbonatites and carbonatites and carbonatites. Canadian Mineralogist 43, 2049–2068.
Mitchell, R.H., Wu, F.-Y., Yang, Y.-H., 2011. In situ U-Pb, Sr and Nd isotopic analysis of loparite by LA-(MC)-ICP-MS. Chemical Geology 280, 191–199.
Moore, K.R., 2012. Experimental study in the Na2O-CaO-MgO-Al2O3-SiO2-CO2 system at 3 GPa: the effect of sodium on mantle melting to carbonate-rich liquids and implications for the petrogenesis of silicocarbonatites. Mineralogical Magazine 76, 285–309.
Moore, M., Chakhmouradian, A., Mariano, A.N., Sidhu, R., 2015. Evolution of Rare-earth Mineralization in the Bear Lodge Carbonatite. In: Ore Geology Reviews 64. Mineralogical and Isotopic Evidence, Wyoming, pp. 499–521.
Nasraoui, M., Waerenborgh, J.C., 2001. Fe speciation in weathered pyrochlore-group minerals from the Lueshe and Araxa (Barreiro) carbonatites by Fe-57 Mossbauer spectroscopy. Canadian Mineralogist 39, 1073–1080.
Nelson, D.R., Chivas, A.R., Chappell, B.W., McCulloch, M.T., 1988. Geochemical and isotopic systematics in carbonatites and implications for the evolution of ocean-island sources. Geochimica et Cosmochimica Acta 52, 1–17.
Olson, J.C., Shawe, D.R., Pray, L.C., Sharp, W.N., 1954. Rare-earth mineral deposits of the mountain Pass district, San Bernardino County, California. U.S. Geological Survey Professional Paper 261.
Oreskes, N., Einaudi, M.T., 1992. Origin of hydrothermal fluids at Olympic Dam: preliminary results from fluid inclusions and stable isotopes. Economic Geology 87, 64–90.
Orris, G.J., Grauch, R.I., 2002. Rare Earth Element Mines, Deposits, and Occurrences. U.S. Geological Survey Open-File Report 2002; 02–189, U.S. Geological Survey, Tucson, AZ.
Palmer, D.A.S., Williams-Jones, A.E., 1996. Genesis of the carbonatite-hosted fluorite deposit at Amba Dongar, India: evidence from fluid inclusions, stable isotopes and whole rock-mineral geochemistry. Economic Geology 91, 934–950.
Peccerillo, A., Lustrino, M., 2005. Compositional variations of the Plio-Quaternary magmatism in the circum-Tyrrhenian area: deep- vs. shallow-mantle processes. In: Foulger, G.R., Natland, J.H., Presnall, D.C., Anderson, D.L. (Eds.), Plates, Plumes and Paradigms, Geological Society of America Special Paper 388, pp. 421–434.
Pekov, I.V., 2000. Lovozero Massif: History, Pegmatites, Minerals. Ocean Pictures Ltd.
Pfaff, K., Krumrei, T., Marks, M., Wenzel, T., Rudolf, T., Markl, G., 2008. Chemical and physical evolution of the 'lower layered sequence' from the nepheline syenitic

Ilímaussaq intrusion, South Greenland: implications for the origin of magmatic layering in peralkaline felsic liquids. Lithos 106, 280–296.
Poitrasson, F., Oelker, E., Schott, J., Montel, J.M., 2004. Experimental determination of synthetic $NdPO_4$ monazite end-member solubility in water from 21 °C to 300 °C: implications for rare earth element mobility in crustal fluids. Geochimica et Cosmochimica Acta 68, 2207–2221.
Pollard, P., 2001. Sodic(–calcic) alteration in Fe-oxide–Cu–Au districts: an origin via unmixing of magmatic H_2O–CO_2–NaCl ± $CaCl_2$–KCl fluids. Mineralium Deposita 36, 93–100.
Potter, J., Rankin, A.H., Treloar, P.J., 2004. Abiogenic Fischer–Tropsch synthesis of hydrocarbons in alkaline igneous rocks; fluid inclusion, textural and isotopic evidence from the Lovozero complex, N.W. Russia. Lithos 75, 311–330.
Pourtier, E., Devidl, J.-L., Gibert, F., 2010. Solubility measurements of synthetic neodymium monazite as a function of temperature at 2 kbars, and aqueous neodymium speciation in equilibrium with monazite. Geochimica et Cosmochimica Acta 74, 1872–1891.
Powell, J.L., Hurley, P.M., Fairbairn, H.W., 1966. The strontium isotopic composition and origin of carbonatites. In: Tuttle, O.F., Gittins, J. (Eds.), Carbonatites. John Wiley & Sons Ltd, pp. 365–378.
Premo, W.R., Moscati, R.J., Cosca, M.A., Stoeser, D., Premo, V.L., 2013. Ages and Pb-Sr-Nd isotopes of silicate rocks at Mountain Pass, Southern California. Geological Society of America *Abstracts with Programs* 45, 113.
Ray, J.S., Ramesh, R., Pande, K., Trivedi, J.R., Shukla, P.N., Patel, P.P., 2000. Isotope and rare earth element chemistry of carbonatite±alkaline complexes of Deccan volcanic province: implications to magmatic and alteration processes. Journal of Asian Earth Sciences 18, 177–194.
Reeve, J.S., Cross, K.C., Smith, R.N., Oreskes, N., 1990. The Olympic Dam copper-uranium-gold-silver deposit, South Australia. In: Hughes, F.E. (Ed.), Geology of the Mineral Deposits of Australia and Papua New Guinea, The Australasian Institute of Mining and Metallurgy, Monograph 14, pp. 1009–1035.
Ren, Y., Zhan, Y., Zhan, Z., 1994. Study on the heat events of ore-forming Bayan Obo deposit. Acta Geoscientia Sinica 1–2, 95–101 (in Chinese with English abstract).
Reynolds, L.J., 2000. Geology of the olympic dam Cu-U-Au-Ag-REE deposit. In: Porter, T.M. (Ed.), Hydrothermal Iron Oxide Copper-gold and Relted Deposits: a Global Perspective. Australian Minerals Foundation, Adelaide, pp. 93–104.
Salvi, S., Williams-Jones, A.E., 1990. The role of hydrothermal processes in the granite-hosted Zr, Y, REE deposit at Strange Lake, Quebec-Labrador – evidence from fluid inclusions. Geochimica et Cosmochimica Acta 54, 2403–2418.
Salvi, S., Williams-Jones, A.E., 1996. The role of hydrothermal processes in concentrating high-field strength elements in the Strange Lake peralkaline complex, northeastern Canada. Geochimica et Cosmochimimica Acta 60, 1917–1932.
Salvi, S., Williams-Jones, A.E., 2006. Alteration, HFSE mineralisation and hydrocarbon formation in peralkaline igneous systems: insights from the Strange Lake Pluton, Canada. Lithos 91, 19–34.
Samoylov, V.S., Kovalenko, V.I., Sengee, D., Ivanov, V.G., Smirnova, Ye.V., Konusova, V.V., Pakhomova, N.N., 1988. Geologic structure, composition, and genesis of a rare earth deposit in Mongolia. Geologiya Rudnykh Mestotozhdeniy 30, 62–74.
Schleicher, H., Keller, J., Kramm, U., 1990. Isotope studies on alkaline volcanics and carbonatites from the Kaiserstuhl, Federal Republic of Germany. Lithos 26, 21–35.
Sheard, E.R., 2010. Behaviour of Zirconium, Niobium, Yttrium and the Rare Earth Elements in the Thor Lake Rare-metal Deposit, Northwest Territories, Canada. Unpublished MSc Thesis. McGill Univeristy, Canada, p. 140.
Sheard, E.R., Williams-Jones, A.E., Heiligman, M., Pederson, C., Trueman, D.L., 2012. Controls on the concentration of zirconium, niobium and the rare earth elements in the Thor Lake rare metal deposit, Northwest Territories, Canada. Economic Geology 107, 81–104.
Simonetti, A., Bell, K., Viladkar, S.G., 1995. Isotopic data from the Amba Dongar carbonatite complex west-central India: evidence for an enriched mantle source. Chemical Geology, Isotope Geoscience 122, 185–198.
Simonetti, A., Goldstein, S.L., Schmidberger, S.S., Viladkar, S.G., 1998. Geochemical and Nd, Pb and Sr isotope data from Deccan alkaline complexes: inferences for mantle sources and plume-lithosphere interaction. Journal of Petrology 39, 1847–1864.
Skirrow, R.G., Bastrakov, E.N., Barovich, K., Fraser, G.L., Creaser, R.A., Fanning, C.M., Raymond, O.L., Davidson, G.J., 2007. Timing of iron oxide Cu-Au-(U) hydrothermal activity and Nd isotope constraints on metal sources in the Gawler craton, South Australia. Economic Geology 102, 1441–1470.
Smith, M.P., Henderson, P., 2000. Preliminary fluid inclusion constraints on fluid evolution in the Bayan Obo Fe-REE-Nb deposit, Inner Mongolia, China. Economic Geology 95, 1371–1388.
Smith, M.P., Spratt, J., 2012. The chemistry of niobium mineralisation at Bayan Obo, Inner Mongolia, China: constraints on the hydrothermal precipitation and alteration of Nb-minerals. Acta Geologica Sinica 86, 700–722.
Smith, M.P., Henderson, P., Zhang, P.S., 1999. Reaction relationships in the Bayan Obo Fe-REE-Nb deposit Inner Mongolia, China: implications for the relative stability of rare-earth element phosphates and fluorocarbonates. Contributions to Mineralogy and Petrology 134, 294–310.
Smith, M.P., Campbell, L.S., Kynicky, J., 2015. A review of the genesis of the world class Bayan Obo Fe–REE–Nb deposits, Inner Mongolia, China: multistage processes and outstanding questions. Ore Geology Reviews 64, 459–476.
Sørensen, H., 1997. The agpaitic rocks – an overview. Mineralogical Magazine 61, 485–498.
Sørenson, H., Bohse, H., Bailey, J.C., 2006. The origin and mode of emplacement of lujavrites in the Ilímaussaq alkalinecomplex, South Greenland. Lithos 91, 286–300.
Staatz, M.H., 1983. Geology and Description of Thorium and Rare-earth Deposits in the Southern Bear Lodge Mountains, North-eastern Wyoming. USGS Professional Paper 1049-D (52 pp.).
Stevenson, R., Upton, B.G.J., Steenfelt, A., 1997. Crust-mantle interaction in the evolution of the Ilimaussaq complex, South Greenland: Nd isotopic studies. Lithos 40, 189–202.
Streckeisen, A., 1976. To each plutonic rock its proper name. Earth-Science Reviews 12, 1–33.
Tao, K., Yang, Z., Zhang, Z., Wang, W., 1998. Systematic geological investigation on carbonatite dykes in Bayan Obo, Inner Mongolia, China. Scientia Geologica Sinica 33, 73–83 (in Chinese with English abstract).
Traversa, G., Gomes, C.B., Brotzu, P., Buraglini, N., Morbidelli, L., Principato, M.S., Ronca, S., Ruberit, E., 2001. Petrography and mineral chemistry of carbonatites and mica-rich rocks from the Araxá complex (Alto Paranaíba Province, Brazil). Anais da Academia Brasileira de Ciencias 73, 71–98.
Thuy, N.T., Wada, H., Ishikawa, T., Shimano, T., 2014. Geochemistry and petrogenesis of carbonatites from South Nam Xe, Lai Chau area, northwest Vietnam. Mineralogy and Petrology 108, 371–390.
Upton, B.G.J., Aspen, P., Hinton, R.W., 2003. Magmatism of the mid-proterozoic Gardar Province, South Greenland: chronology, petrogenesis and geological setting. Scottish Journal of Geology 39, 169–184.
Upton, B.G.J., Macdonald, R., Odling, N., Ramo, O.T., Baginski, B., 2013. Kungnat, revisited. A review of five decades of research into an alkaline complex in South Greenland, with new trace-element and Nd isotopic data. Mineralogical Magazine 77, 523–550.
USGS, 2015. Mineral resources on line spatial data. http://mrdata.usgs.gov/ree/show-ree.php?rec_id=174.
US Department of Energy, 2011. Critical Metals Strategy. US Department of Energy, p. 196.
Varga, Z., Wallenius, M., Mayer, K., Keegan, E., Millett, S., 2009. Application of lead and strontium isotope ratio measurements for the origin assessment of uranium ore concentrates. Analytical Chemistry 81, 8327–8334.
Vasyukova, O., Williams-Jones, A.E., 2014. Fluoride–silicate melt immiscibility and its role in REE ore formation: evidence from the Strange Lake rare metal deposit, Quebec-Labrador, Canada. Geochimica et Cosmochimica Acta 139, 110–130.
Veksler, I.V., Dorfman, A.M., Dulski, P., Kamenetsky, V.S., Danyushevsky, L.V., Jeffries, T., Dingwell, D.B., 2012. Partitioning of elements between silicate melt and immiscible fluoride, chloride, carbonate, phosphate and sulfate melts, with implications to the origin of natrocarbonatite. Geochimica et Cosmochimica Acta 79, 20–40.
Viladkar, S.G., 1981. The carbonatites of Amba Dongar, Gujarat, India. Bulletin of the Geological Society of Finland 53, 17–28.
Viladkar, S.G., Schidlowski, M., 2000. Carbon and oxygen isotope geochemistry of the Amba Dongar carbonatite complex, Gujarat, India. Gondwana Research 3, 415–424.
Vladykin, N.V., Kotov, A.B., Borisenko, A.S., Yarmolyuk, V.V., Pokhilenko, N.P., Salnikova, E.B., Travin, A.V., Yakovleva, S.Z., 2014. Age boundaries of formation of the Tomtor alkaline-ultramafic pluton: U-Pb and $^{40}Ar/^{39}Ar$ geochronological studies. Doklady Earth Sciences 454, 7–11.
Waight, T., Baker, J., Willigers, B., 2002. Rb-isotope dilution analyses by MC-ICPMS using Zr to correct for mass fractionation. Chemical Geology 186, 99–116.
Wakita, H., Rey, P., Schmidt, R.A., 1971. Abundances of the 14 rare-earth elements and 12 other trace elements in Apollo 12 samples: five igneous and one breccia rocks and four soils. Proceedings of the Second Lunar Science Conference. Geochimica et Cosmochimica Acta Supplement 2, 1319–1329.
Wall, F., 2014. Rare earth elements. In: Gunn, Gus (Ed.), Critical Metals Handbook. Wiley-Blackwell, pp. 312–339.
Wall, F., Mariano, A.N., 1996. Rare earth minerals in carbonatites: a discussion centred on the Kangankunde carbonatite, Malawi. In: Jones, A.P., Wall, F., Williams, C.T. (Eds.), Rare Earth Minerals: Chemistry, Origin and Ore Deposits. Chapman and Hall, London, UK.
Wallace, M.E., Green, D.H., 1988. An experimental determination of primary carbonatite magma composition. Nature 335, 343–346.
Wang, J.W., Tatsumoto, M., Li, X.B., Premo, W.R., Chao, E.C.T., 1994. A precise ^{232}Th-^{208}Pb chronology of fi ne-grained monazite: age of the Bayan Obo REE-Fe-Nb ore deposit, China. Geochimica et Cosmochimica Acta 58, 3155–3169.
Wedepohl, K.H., 1995. The composition of the continental crust. Geochimica et Cosmochimica Acta 59, 1217–1232.
Williams, P.J., Barton, M.D., Johson, D.A., Fontbote, L., de Haller, A., Mark, G., Oliver, N.H.S., Marschik, R., 2005. Iron oxide copper-gold deposits: geology, space-time distribution, and possible modes of origin. Economic Geology 100, 371–405.
Williams-Jones, A.E., Palmer, D.A.S., 2001. The evolution of aqueous–carbonic fluids in the Amba Dongar carbonatite, India: implications for fenitisation. Chemical Geology 185, 283–301.
Williams-Jones, A.E., Migdisov, A.A., Samson, I.M., 2012. Hydrothermal mobilisation of the rare earth elements – a Tale of "Ceria" and "Yttria". Elements 8, 355–360.
Wood, S.A., 1990. The aqueous geochemistry of the rare earth elements and yttrium. Part I. Review of available low temperature data for inorganic complexes and the inorganic REE speciation of natural waters. Chemical Geology 82, 159–186.

Wood, S.A., 1993. The aqueous geochemistry of the rare earth elements: critical stability constants for complexes with simple carboxylic acids at 25 °C and 1 bar and their application to nuclear waste management. Journal of Geological Engineering 34, 229–259.

Wood, S.A., Williams-Jones, A.E., 1994. The aqueous geochemistry of the rare-earth elements and yttrium 4. Monazite solubility and REE mobility in exhalative massive sulfide-depositing environments. Chemical Geology 115, 47–60.

Woolley, A.R., 1986. Alkaline Rocks and Carbonatites of the World – Part 1: North and South America. Britich Museum (Natural History), London, p. 216.

Woolley, A.R., Bailey, D.K., 2012. The crucial role of lithospheric structure in the generation and release of carbonatites: geological evidence. Mineralogical Magazine 76, 259–270.

Woolley, A.R., Church, A.A., 2005. Extrusive carbonatites: a brief review. Lithos 85, 1–14.

Wu, C., 2008. Bayan Obo Controversy: Carbonatites versus Iron Oxide-Cu-Au-(REE-U). Resource Geology 58, 348–354.

Wyllie, P.J., Tuttle, O.F., 1960. The system CaO-CO_2-H_2O and the origin of carbonatites. Journal of Petrology 1, 1–46.

Wyllie, P.J., Jones, A.P., Deng, J., 1996. Rare earth elements in carbonate-rich melts from mantle to crust. 77–103. In: Jones, A.P., Wall, F., Williams, C.T. (Eds.), Rare Earth Minerals: Chemistry, Origin and Ore Deposits. Mineral. Soc. Series, 7.

Xu, C., Huang, Z.-L., Liu, C.-Q., Qi, L., Li, W.-B., Guan, T., 2003. Sources of ore-forming fluids in the Maoniuping REE deposit, Sichuan Province, China: evidence from REE, radiogenic Sr, Nd, and stable isotopes studies. International Geology Review 45, 635–645.

Xu, C., Kynicky, J., Chakhmouradian, A.R., Campbell, I.H., Allen, C.M., 2010. Trace element modelling of the magmatic evolution of rare-earth-rich carbonatite from the Miaoya deposit, Central China. Lithos 118, 145–155.

Yang, K.F., Fan, H.R., Santosh, M., Hu, F.F., Wang, K.Y., 2011. Mesoproterozoic carbonatitic magmatism in the Bayan Obo deposit, Inner Mongolia, North China: constraints for the mechanism of super accumulation of rare earth elements. Ore Geology Reviews 40, 122–131.

Zaitsev, A.N., Wall, F., Le Bas, M.J., 1998. REE-Sr-Ba minerals from the Khibina carbonatites, Kola Peninsula, Russia: their mineralogy, paragenesis and evolution. Mineralogical Magazine 62, 225–250.

Zhang, Z.Q., Yuan, Z.X., Tang, S.H., Bai, G., Wang, J.H., 2003. Age and Geochesmistry of the Bayan Obo Ore Deposit. Geological Publishing House, Beijing, p. 205 (in Chinese with English abstract).

Zindler, A., Hart, S., 1986. Chemical geodynamics. Earth and Planetary Science Letters 14, 493–571.